



ČESKÉ VYSOKÉ UČENÍ TECHNICKÉ V PRAZE

Fakulta elektrotechnická
Katedra elektromagnetického pole

Excitation of Conducting Cylinder Using Slots

Diploma Thesis

Study program: Communications, multimedia and electronics
Study field: Communication systems

Thesis supervisor: doc. Ing. Pavel Hazdra, Ph.D.

Anita Pascawati

Praha 2017

I. OSOBNÍ A STUDIJNÍ ÚDAJE

Příjmení: **Pascawati** Jméno: **Anita** Osobní číslo: **452837**
Fakulta/ústav: **Fakulta elektrotechnická**
Zadávající katedra/ústav: **Katedra teorie obvodů**
Studijní program: **Komunikace, multimédia a elektronika**
Studijní obor: **Komunikační systémy**

II. ÚDAJE K DIPLOMOVÉ PRÁCI

Název diplomové práce:

Excitation of Conducting Cylinder Using Slots

Název diplomové práce anglicky:

Excitation of Conducting Cylinder Using Slots

Pokyny pro vypracování:

Use the Theory of Characteristic Modes (CM) to find first few modes (2-3 in total) of conducting cylinder of given length to radius ratio. Determine its properties: resonant frequency, bandwidth potential, shape of the current, radiation pattern. Decide where to put slots in order to excite at least two modes independently. Model the structure with EM simulator, evaluate input impedances and design required matching circuits. Verify the design by measurement.

Seznam doporučené literatury:

- [1] Y. Chen, Ch. Wang, Characteristic Modes: Theory and Applications in Antenna Engineering, Wiley, 2015
- [2] R. Martens, D. Manteuffel, "A Feed Network for the Selective Excitation of Specific Characteristic Modes on Small Terminals", EuCAP 2011

Jméno a pracoviště vedoucí(ho) diplomové práce:

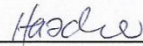
doc. Ing. Pavel Hazdra Ph.D., katedra elektromagnetického pole FEL

Jméno a pracoviště druhé(ho) vedoucí(ho) nebo konzultanta(ky) diplomové práce:

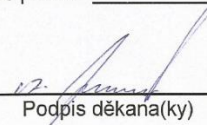
Datum zadání diplomové práce: **02.03.2017**

Termín odevzdání diplomové práce: _____

Platnost zadání diplomové práce: **30.09.2018**


Podpis vedoucí(ho) práce

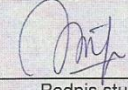

Podpis vedoucí(ho) ústavu/katedry


Podpis děkana(ky)

III. PŘEVZETÍ ZADÁNÍ

Diplomantka bere na vědomí, že je povinna vypracovat diplomovou práci samostatně, bez cizí pomoci, s výjimkou poskytnutých konzultací. Seznam použité literatury, jiných pramenů a jmen konzultantů je třeba uvést v diplomové práci.

13. 03. 2017
Datum převzetí zadání


Podpis studentky

Honorable statement

"I declare that I have prepared the submitted thesis independently and that I have provided all the information resources used in accordance with the Methodological Guideline on Ethical Principles in the Preparation of Higher Education."

Date: 26.5.2017

Anita Pascawati

ACKNOWLEDGMENT

First of all, I am grateful to Allah SWT for His mercy upon me, assistance, strength, and good health in order to complete this master thesis.

I am very thankful to my parents, my brother, and family who always provide full of love, support, and pray for me and for the successful of this work.

I would like to express my deepest gratitude for my supervisor, doc. Ing. Pavel Hazdra, Ph.D., for his brilliant idea, guidance, encouragement, and mentorship throughout this project, also for his pleasant manner.

My thanks also belong to the Department of Electromagnetic Field and staffs for the cooperation in the implementation of the proposed designed and the acquisition of data for the practical part of the work.

ABSTRACT

This master thesis deals with the investigation to excite the conducting cylinder of rocket chassis using slots. The theory of characteristic mode (TCM) is used to find the resonance modes of the cylinder. The model of conducting cylinder is designed and simulated in FEKO software to obtain the resonance modes. Furthermore, the cylinder with two selected modes excitation are designed and simulated in CST software. The excitation of the modes are achieved by mounting the H-shaped slots on the cylinder at the specific location where the maximum currents distribution taken place. Due to the reactive of load impedance, the L-matching networks and transmission line using coaxial cable are utilized to match it to the input impedance. Finally, the proposed concept are verified by manufacturing and measurement. It is shown that the results of measurement are in excellent agreement with the simulation. Hence, it is confirmed that in this research, the proposed idea is successfully designed and implemented.

Index Terms: Conducting cylinder, rocket chassis, theory of characteristic modes (TCM), H-shaped slots, excitation of modes, L-matching networks, coaxial cable.

Table of Contents

List of Tables	viii
List of Figures	ix
List of Symbols and Abbreviations.....	x
Chapter 1.....	1
Introduction	1
Chapter 2.....	2
The Theory of Characteristic Modes (TCM)	2
Chapter 3.....	4
The Characteristic Modes of Conducting Cylinder.....	4
3.1 The Characteristic Modes Simulation of Cylinder	4
3.2 The Characteristic Modes of Different Thickness of Cylinder	7
3.3 The Characteristic Modes of Different Ratio of Open Cylinder	7
3.4 Quality Factor	8
Chapter 4.....	9
Excitation Of Modes	9
4.1 Inductive Coupling Excitation	9
4.2 Excitation Using H-Shaped Slots.....	9
Chapter 5.....	13
Simulation Results.....	13
5.1 Surface Currents	14
5.2 Radiation Patterns	15
Chapter 6.....	16
Feeding System of Slots	16
6.1 L-Matching Network.....	16
6.2 Cable Impedance	18
Chapter 7.....	24
Manufacturing of Proposed Design And Measurement.....	24
7.1 Fabricated Cylinder.....	24
7.2 Measurement of Fabricated Cylinder	25

Chapter 8.....	27
Conclusion	27
References	29
Appendix	30

List of Tables

Table 1. List of important symbols	x
Table 2. List of abbreviations	x
Table 3. Quality factor of characteristic modes.....	8
Table 4. Models of slot and their impedance	10
Table 5. Calculation value for excitation modes in the first configuration	21
Table 6. Calculation value for excitation modes in the second configuration	22
Table 7. Calculation value for excitation modes in the third configuration.....	23

List of Figures

Fig. 1. Characteristic modes of the conducting cylinder with diameter 0.1 m and length 1 m	4
Fig. 2. Variation of the characteristic angle with frequency, for the first ten characteristic modes of the conducting cylinder with diameter 0.1 m and length 1 m	6
Fig. 3. Dimension of H-Shaped Slot.....	11
Fig. 4. Mounting H-Shaped Slot on Cylinder	12
Fig. 5. Impedance of cylinder ports	13
Fig. 6. Distribution current along the H-shaped slot	14
Fig. 7. Surface currents from simulation results.....	14
Fig. 8. Radiation Pattern of cylinder	15
Fig. 9. Movement of adding reactive components on smith chart	17
Fig. 10. Four possible matching network for modes 1 and 7	17
Fig. 11. First configuration of matching networks for mode 1.....	19
Fig. 12. First configuration of matching networks for mode 7	20
Fig. 13. Second configuration of matching networks	21
Fig. 14. Third configuration of matching networks	23
Fig. 15. Fabricated cylinder	24
Fig. 16. Soldering of capacitors and coaxial cables.....	25
Fig. 17. Measurement of fabricated cylinder in the anechoic chamber	26
Fig. 18. S-Parameter results between simulation and measurement.....	26

List of Symbols and Abbreviations

Table 1. List of important symbols

λ_n	Eigenvalue of a characteristic mode
J_n	Characteristic current
Z	Impedance matrix
E_n	Characteristic electrical field
α_n	Characteristic angle
λ_0	Wavelength in the vacuum
λ_g	Wavelength in the transmission line
f	Resonant frequency
c	Speed of the light
H_n	Magnetic fields
Q_n	Quality factor of characteristic mode
$\partial\omega$	Bandwidth of resonant frequency
$\partial\lambda$	Eigenvalue width
δ_{mn}	Kronecker Delta
L_v	Length of vertical arms of the H-shaped slot
W_v	Width of vertical arms of the H-shaped slot
L_h	Length of horizontal arms of the H-shaped slot
W_h	Width of horizontal arms of the H-shaped slot
L	Cable length
Z_0	Characteristic impedance
Z_L	Load impedance
ϵ_r	Relative dielectric constant of the cable
Z_{IN}	Input impedance
RL	Return loss
BW	Bandwidth
f_2	Upper band frequency
f_1	Lower band frequency
Q	Quality factor of antenna

Table 2. List of abbreviations

TCM	Theory of Characteristic Modes
ICE	Inductive coupling element

Chapter 1

INTRODUCTION

Nowadays, research in the antennas field continues to grow. The development of antennas for communication system of rocket becomes interesting part in this field. The performance of antennas for rocket is really important to ensure that transmission of telemetry data from the rocket can reach the ground stations. However, the antennas should not disturb aerodynamics of rocket. Therefore, different kind of antennas for rocket application have been investigated in several research. The detailed explanation respecting to aerodynamic analysis is out of the scope of this research. Despite of mounting antennas on the rockets body, it is a good idea to excite the rocket chassis itself acting as an effective radiator. The inspiration comes from the technology of mobile phone which utilizes the chassis of its PCB as antenna. The rocket chassis which is made from steel is a perfectly conducting material. The theory of characteristic mode (TCM) can be used to find the resonance modes of the cylinder of rocket. The modes have orthogonal radiation patterns which is good for the tracking system. The tracking of rocket sometime require the use of several radio frequencies of transmitter/transponder. By using several orthogonal modes for excitation of chassis rocket, the tracking of rocket from different ground stations can be performed.

The theory of characteristic modes is developed by Garbacz [1] and refined by Harrington and Mautz [2]. Characteristic modes theory is utilized to obtain the radiating modes of arbitrarily shaped perfectly conducting (PEC) material. The conducting material is associated with the scattering of characteristic currents on the surface of its body. Characteristic currents radiates the characteristic electric fields into the free space. There is a phase lag between the characteristic currents and characteristic fields called characteristic angle that indicates the resonant frequency of each mode [3].

In this master thesis, the model of rocket of conducting cylinder is designed. FEKO software [4] is used to obtain the characteristic modes of the conducting cylinder. The modes that can be effectively used for radiation are determined. Also, the way of how to excite them are investigated. Furthermore, the excitation of modes are conducted by utilizing the inductive coupling elements. The excitation is implemented by mounting the H-shaped slots on the cylinder to excite the modes. The H-shaped slots are designed with regard to obtain high real part impedance of cylinder. The cylinder with the mounted slots is designed and simulated in CST software [5]. After that, the matching network for each mode are designed to match the input impedance of cylinder to 50 ohm. Several schemes of L-matching network that can be used for matching are investigated. Furthermore, the simulation results are evaluated and optimized. Finally, the proposed design is verified by the fabrication and measurement.

Chapter 2

The Theory of Characteristic Modes

The characteristic modes can be defined as a method to characterize the surface current and radiated fields behavior of the conducting bodies of arbitrary shapes. The characteristic modes can be described into the following eigenvalues λ_n equation [2]:

$$\mathbf{X}(\mathbf{J}_n) = \lambda_n \mathbf{R}(\mathbf{J}_n) \quad (1)$$

Where \mathbf{J}_n are the characteristic currents or eigencurrents and n is the order index of each mode. \mathbf{J}_n and λ_n should be real since both \mathbf{R} and \mathbf{X} are the real symmetric operators. The characteristic currents have to be orthogonal to each other that is discussed in [2] and [3]. Furthermore, \mathbf{R} and \mathbf{X} represent the real and imaginary parts of the impedance matrix \mathbf{Z} , respectively, those are given by [2]:

$$\mathbf{Z} = \mathbf{R} + j\mathbf{X} \quad (2)$$

The characteristic currents \mathbf{J}_n on the surface of a PEC body only depend on its size and shape and not on any specific excitation [6].

The eigencurrents on the surface of conducting body produce electric fields which is called characteristic fields or eigenfields \mathbf{E}_n . This characteristic fields have orthogonality relationships which is reduced to the following equation [2]:

$$\omega \iiint (\mu \mathbf{H}_m \cdot \mathbf{H}_n^* - \varepsilon \mathbf{E}_m \cdot \mathbf{E}_n^*) d\tau = \lambda_n \delta_{mn} \quad (4)$$

Where \mathbf{H}_n is the magnetic fields produced by the currents, ω is the resonant frequency, δ_{mn} is the Kronecker delta (0 for $m \neq n$, and 1 for $m = n$), μ and ε are permeability and permittivity of free space, respectively.

Equation (4) defines that the difference between magnetic and electric field energy in radiation is comparable to the eigenvalues magnitude. It is the way to show the associated mode that is near resonance. In the case of $\lambda_n = 0$, most of field energy are radiated and it indicates that the associated modes are the resonant modes. In the case of $\lambda_n > 0$, the stored energy of magnetic field greater than the electric field and it indicates that the associated modes are the inductive modes. In the case of $\lambda_n < 0$, the stored energy of electric field greater than the magnetic field and it indicates that the associated modes are the capacitive modes [3].

There exist a phase lag between the current \mathbf{J}_n and tangential electrical field \mathbf{E}_n^{tan} on PEC surface that known as characteristic angle α_n and defined by [3]:

$$\alpha_n = 180^\circ - \tan^{-1} \lambda_n \quad (5)$$

The characteristic angle is determined from the associated of eigenvalue. The characteristic angle that varies with frequency describe the radiation or scattering ability of the associated

mode. The characteristic angle information can be used to determine which modes can be used for radiation and excitation.

The characteristic angles varies in the range 90° to 270° . Corresponding to the characteristic modes, the variation of the characteristic angles are used to describe the resonant behavior of each modes. In the case of $\alpha_n = 180^\circ$, the mode is a good radiator and it indicates that the associated modes are resonant modes. In the case of $\alpha_n = 90^\circ - 180^\circ$, the mode mainly stores magnetic field energy and it indicates that the associated modes are inductive modes. In the case of $\alpha_n = 180^\circ - 270^\circ$, the mode mainly stores electric field energy and it indicates that the associated modes are capacitive modes [3].

The Characteristic Modes of Conducting Cylinder

In this master thesis, the characteristic modes of metallic cylinder are computed by using FEKO software. For simulation purposes, the models of rocket cylinder from PEC are designed. The design of conducting cylinder is derived from a pipe with the length, $L = 1\text{ m}$, and diameter, $d = 0.1\text{ m}$.

3.1 The Characteristic Modes Simulation of Cylinder

Simulation results show that conducting cylinder has two modes that are good for excitation, i.e., modes 1 and 7. The modes have characteristic currents that behave like a dipole as depicted in Fig 1.

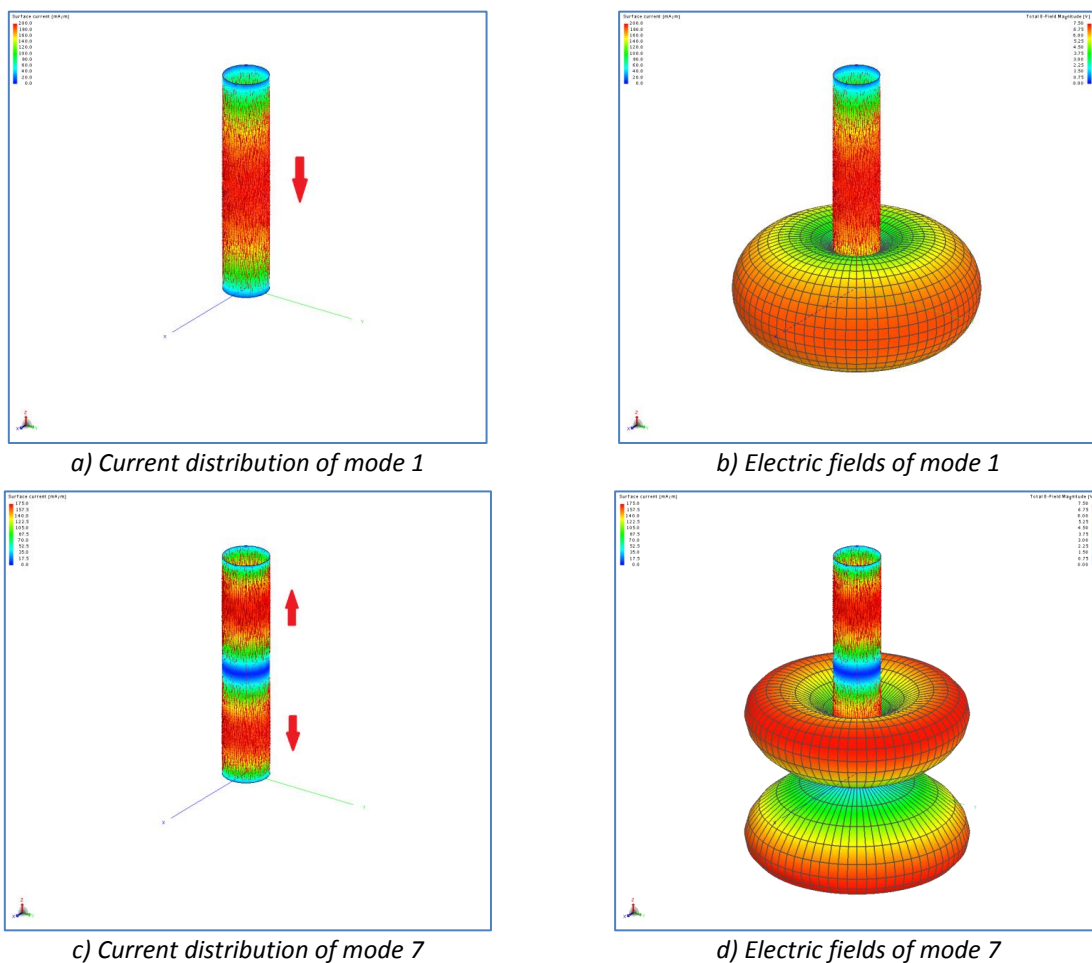


Fig. 1. Characteristic modes of the conducting cylinder with diameter 0.1 m and length 1 m

The characteristic currents of mode 1 describes the current distribution of a half wavelength dipole with the maximum currents at the centre of cylinder as shown in Fig. 1a. While the characteristic currents of mode 7 represent the current distribution of one wavelength dipole with the two specific maximum current at the surface of cylinder as shown in Fig. 1c.

The electric currents on the surface of conducting cylinder produce the electric fields of excitation modes. There are different distributions of the electric current between two modes that generates different radiation pattern of electric fields. Mode 1 has maximum current distribution in one direction along the cylinder surface radiating the characteristic fields representing omnidirectional radiation pattern as shown in Fig. 1b. On the contrary, since the electric currents flowing in the two opposite directions, mode 7 has different radiation pattern as depicted in Fig. 1d.

Fig. 2 shows the characteristic modes for conducting cylinder with $d = 0.1 \text{ m}$ and $L = 1 \text{ m}$. It presents the variation of the characteristic angles with frequency. When the characteristic angles close to 180° , it indicates that the associated modes are resonant modes. From 10 computed of characteristic modes, there are five modes that have resonant mode, i.e., mode indexes 1, 2, 3, 7, and 9.

It can be seen from the Fig. 2 that modes 1 and 7 resonate at frequency 126 MHz and 285 MHz, respectively. It should be noted that since the cylinder behaves as a dipole, if the length of cylinder is equal to a half wavelength, e.g., $\lambda/2 = 1 \text{ m}$, the resonant frequency of mode 1 should be 150 MHz. However, this is the resonant frequency for thin dipole. Since the conducting cylinder describing a thick dipole, therefore mode 1 resonates at the lower frequency. On the other hand, the resonant frequency of mode 7 represents the resonant frequency of one wavelength dipole. Hence, if the length of cylinder is equal to one wavelength, e.g., $\lambda = 1 \text{ m}$, the resonant frequency should be 300 MHz. Similar to the case of mode 1, since the cylinder is thicker than a dipole, therefore mode 7 has lower resonant frequency.

There are three other modes that also have resonances. Mode indexes 2 and 3 resonate at the same frequency 872 MHz and mode index 9 resonates at 841 MHz. These characteristic modes can be seen in the appendix (Ap. 4 – 6). The modes have several maximum currents distribution at specific location and have radiation pattern with many sidelobes showing the directivity of cylinder at higher frequencies. The other modes do not resonate and present either inductive or capacitive behavior in the range frequency of 100 MHz – 1 GHz.

Between five resonance modes, modes 1 and 7 have characteristic modes that can be excited more effectively. Therefore, in this master thesis, the details investigation is performed only for these two selected resonance modes.

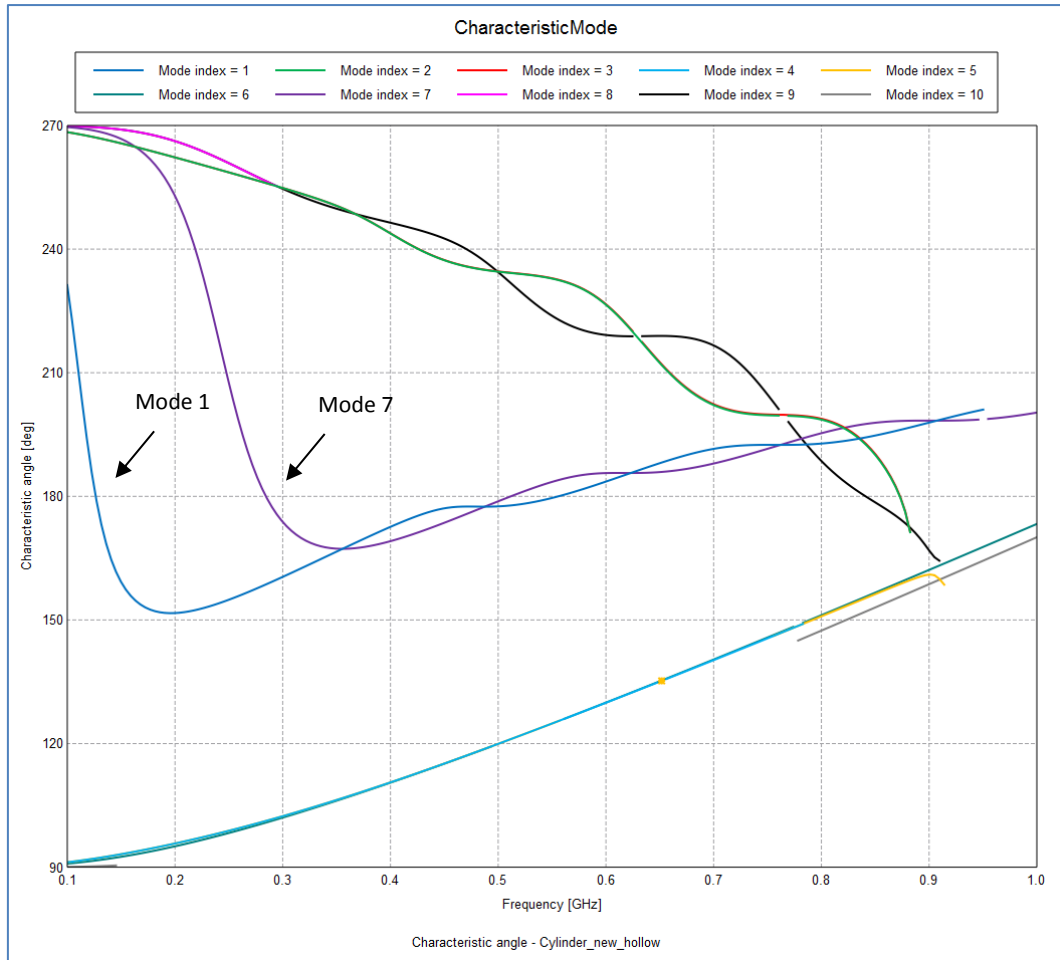


Fig. 2. Variation of the characteristic angle with frequency, for the first ten characteristic modes of the conducting cylinder with diameter 0.1 m and length 1 m.

It is explained from [7] that the eigencurrents J_n can be excited more effectively near their resonant frequencies. The current distribution of each characteristic modes has the maximum and minimum at specific locations. Since having different phase 180° , the minimum of electric field distribution will be located at the maximum of current distribution. Hence, the use of inductive coupler at the maximum of current distribution can excite the characteristic modes.

The characteristic current of mode 1 flows in one direction from the upper cylinder to the lower cylinder with its maximum current at the centre of cylinder. In this case, the mode 1 can be excited by inductive coupler at the centre of cylinder. The characteristic current of mode 7 flow in two opposite direction with two specific maximum current at the surface of cylinder. In this case, the mode can be excited by two inductive coupler in the specific location where the currents are maximum with different phase 180° respectively.

3.2 The Characteristic Modes of Different Thickness of Cylinder

The simulation of TCM is performed for open cylinder (with hole) and closed cylinder (without hole) with $d = 0.1 \text{ m}$ and $L = 1 \text{ m}$, to show the difference between these two structures. The cylinder with the hole excite 5 resonance modes, while the closed cylinder excite only two resonance modes, i.e. modes 1 and 7, that resonate at frequency 123 MHz and 277 MHz. The characteristic modes of closed cylinder are shown in the appendix (Ap. 1 – 3)

The characteristic modes of closed cylinder structure have similar resonant behavior with the same indexes from open cylinder structure. Nevertheless, the open cylinder structure compute more different modes than the closed cylinder structure. There exist internal resonances, inside the cylinder, which can affect the number of available modes. This computation shows that cylinder with length 1m and diameter 0.1 m has two effective resonance modes that can be excited, without concerning the thickness of structure. In the following chapter, only two modes from the open cylinder structure that are investigated.

3.3 The Characteristic Modes of Different Ratio of Open Cylinder

The simulation for open cylinder is conducted in several diameter, i.e., 0.1, 0.2, and 0.3 m, for the same length 1 m. Therefore, it can be analyzed how is the characteristic modes behavior for the different diameter of cylinder. In each simulation, only the first ten characteristic modes are considered.

The open cylinder with $d = 0.2 \text{ m}$ and $L = 1 \text{ m}$ has five resonant modes. Modes indexes 1, 8 and 9 resonates at frequency 134 MHz, 448 MHz, and 449 MHz, respectively. While mode indexes 2 and 3 resonate at the same frequency 414 MHz. Mode 1 has similar characteristic currents with the same mode of open cylinder with diameter 0.1 m, also the characteristic fields are the same. However, the other modes are different that they represent the resonant frequency of 1.5 wavelength dipole. The currents distribution have more specific positions of maximum current and hence they have radiation pattern with several lobes. These modes can be seen in the appendix (Ap. 7 – 12) for more details.

The characteristic modes of closed cylinder with $d = 0.3 \text{ m}$ and $L = 1 \text{ m}$ has four resonant modes. Mode indexes 2 and 3 resonate at frequency 287 MHz, while mode indexes 7 and 8 resonate at frequency 321 MHz. The modes describe one wavelength and 1.25 wavelength resonant mode with slightly different current distribution. The modes are shown in the appendix (Ap. 13 – 17).

Based on the investigation, the differences of diameter of cylinder perform different characteristic modes. Also, the resonant frequency of each mode is different. Note that each mode should be excited in the different ways depend on its current distribution. In addition, the coupler is put at the maximum current position of each mode.

3.4 Quality Factor

A quality factor is a parameter that can be used to measure a broadband behavior of the scatterer, in order to know the bandwidth potential of each modes. The quality factor Q_n of resonant modes is defined as [8]:

$$Q_n = \omega \frac{\partial \lambda}{\partial \omega} \quad (6)$$

where $\partial \omega$ is bandwidth of resonant frequency and $\partial \lambda$ is eigenvalue width.

The calculations of quality factor for each mode of the cylinder with diameter 0.1 m and length 1 m are shown in Table 3. Note that quality factor contributes to the scattered field and describes the scatterer type [8]. The resonant modes with lower Q_n in the case of modes 1, 7, and 9 indicate the broadband scatterer. While higher Q_n in the case of modes 2 and 3 indicate the narrowband scatterer. From point of view the quality factor, modes 1 and 7 of this cylinder have broadband of range frequency that are good to be excited.

Table 3. Quality factor of characteristic modes

Characteristic modes	Resonant Frequency [MHz]	Bandwidth [MHz]	$\partial \lambda$	Quality Factor
1	126	6.8	0.17	3.15
2	872	5.8	0.07	10.12
3	872	6.2	0.07	10.24
7	285	25.6	0.21	2.38
9	841	18.8	0.05	2.47

The simulation results show that two modes of open cylinder with $d = 0.1 \text{ m}$ and $L = 1 \text{ m}$ are effective to be excited, i.e., modes 1 and 7 with the resonant frequency of 126 MHz and 285 MHz, respectively. The excitation of mode 1 can be conducted by one inductive coupler at the centre of cylinder, while mode 7 can be excited by using two inductive coupler at the maximum current position having different phase of 180° . Due to the orthogonality of characteristic fields, these two modes can be excited together for multiband transmission purposes.

Chapter 4

EXCITATION OF MODES

In this master thesis, the excitation of two modes of conducting cylinder is investigated. These two modes, 1 and 7, are obtained using the theory of characteristic modes discussed in the previous sections. The excitation can be conducted by using inductive coupling elements (ICE). Based on the investigations in [9], ICEs are realized by mounting the small rectangular loops at the edges of rectangular PCB, where the maximum of characteristic current distributions take place. ICEs excite the current distributions on the arms of the loop. Also, the same currents are flowing on the wider track.

4.1 Inductive Coupling Excitation

By using the same approach as in [9] and [10], in this master thesis ICEs are realized by mounting the slots at conducting cylinder, where the current distributions are maximum. The slots excite the current distributions on the surface of conducting cylinder. The strongest currents occur in the inner edge of the slots and spread further to the whole cylinder's surface.

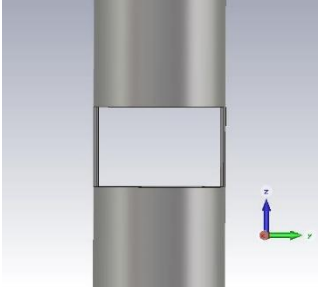
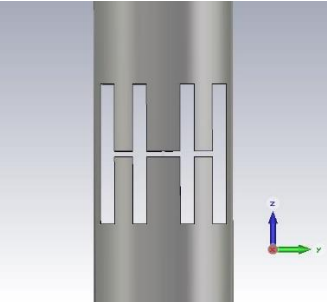
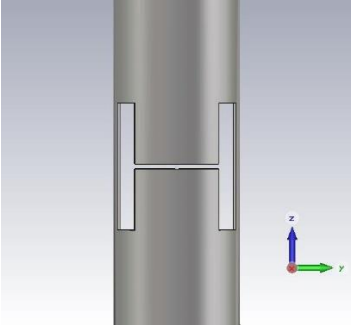
Excitation of the conducting cylinder having slots is performed by using CST simulator [5]. For simulation purposes, the PEC cylinder with the length of 1 m and the diameter of 0.1 m are designed. Two different modes are excited on the cylinder. Mode 1 works at resonant frequency 126 MHz and the current distribution of this mode represent a half wavelength of dipole with the maximum currents are at the centre of cylinder. Excitation of mode 1 is realized by exciting two slots in phase. Mode 7 works at resonant frequency 285 MHz and the current distribution of this mode represent one wavelength of dipole with the two specific maximum current at the surface of cylinder. Excitation of mode 7 is conducted by exciting two of four slots in phase and the other two are 180° out of phase.

4.2 Excitation Using H-Shaped Slots

Shape and dimension of slots are designed with respect to obtain the high real part impedance of cylinder. In the simulation, cylinder with some shape of cutting of slots are calculated, e.g. common rectangular slot, multi-arms folded slot, and one pair folded slot (H-shaped slot). Based on the results, H-shaped slot has higher impedance with smaller size than other shapes. The rectangular slot requires a big size to obtain higher impedance. On the other hand, multi-arms folded slot requires some of vertical arms to obtain better impedance which is not compact from mechanical point of view. Therefore, H-shaped slot is a preferable coupler design

viewed from impedance value and compactness. The different shape of slots and their impedance are shown in Table 4.

Table 4. Models of slot and their impedance

Models of Slot	Self impedance of Cylinder
 <p data-bbox="391 835 608 869">Rectangular Slot</p>	$Z_{in} = 2.38 + j75.32 \Omega$
 <p data-bbox="349 1294 649 1328">Multi-arms Folded Slot</p>	$Z_{in} = 2.29 + j56.03 \Omega$
 <p data-bbox="405 1776 593 1809">H-Shaped Slot</p>	$Z_{in} = 2.69 + j44.36 \Omega$

The shape and dimension of slots are determined by tuning their length and width to improve the cylinder impedance. An H-shaped slot is introduced here in order to obtain the high real

part of cylinder impedance with as smallest slot as possible. The higher cylinder impedance easier to be matched to 50Ω . Smaller size of slot is prefer due to aerodynamics of rocket purposes and compactness for mechanical process. It can be seen from Fig. 3, H-shaped slot has length and width of the vertical arms, $L_v = 100 \text{ mm}$ and $W_v = 23 \text{ mm}$, length and width of the horizontal arms, $L_h = 72 \text{ mm}$ and $W_h = 4 \text{ mm}$, and $L_a = 48 \text{ mm}$. The longer either L_v or L_h , the higher the impedance is. The wider W_v , the higher the impedance as well. Contrarily with the W_h , more narrow the width, the higher the impedance is achieved, so that W_h is designed with very narrow size. Despite of considering the cylinder impedance, design of slot also respects to the current distribution of each mode. From TCM simulation, current distribution of each mode is flowing along the length of cylinder. For more details, the surface current of designed slot is discussed in the simulation results section.

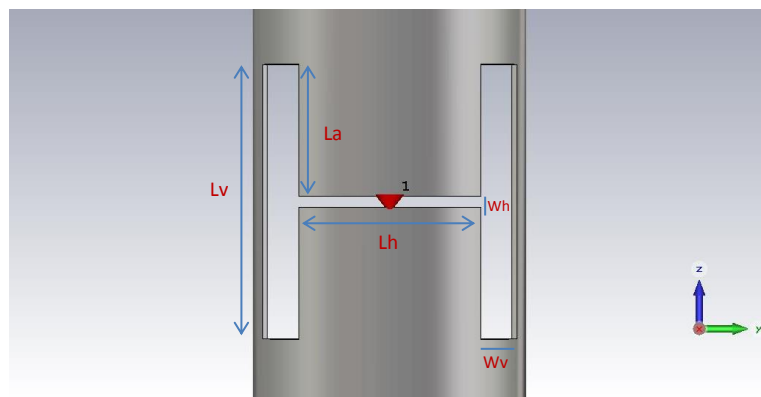
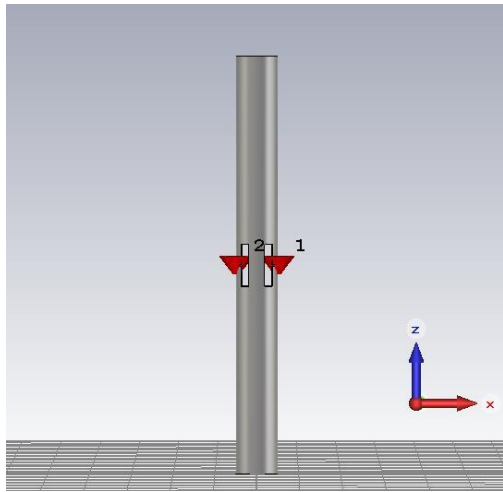
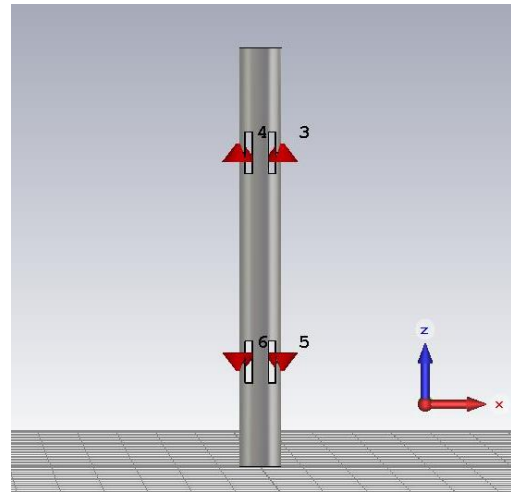


Fig. 3. Dimension of H-Shaped Slot.

Structure of cylinder with H-slots cutting are designed in CST software for simulation purpose. Mode 1 is excited using two H-shaped slots which are mounted at the middle of cylinder in opposite sides. While mode 7 is excited using two opposite H-shaped slots at the upper part and two opposite H-shaped slots in the lower part of cylinder. In the simulation, it is shown that the different phase between two pairs of slots are performed by creating port in 180° different direction. The structure cylinder in modes 1 and 7 are depicted in Figs. 4a and 4b, respectively. By using this H-shaped slot for excitation, modes 1 and 7 have each port impedance of $Z_{ant,mode1} = 2.69 + j44.36 \Omega$ and $Z_{ant,mode2} = 17.39 + j129.22 \Omega$, respectively.



(a) Mode 1



(b) Mode 7

Fig. 4. Mounting H-Shaped Slot on Cylinder.

5.1 Surface Currents

The currents flowing on the surface of cylinder are simulated in CST software by considering the phase between ports. To excite the currents of mode 1, the ports 1 and 2 should be powered in the same phase. The other different way is conducted to excite the currents of mode 7, that the ports 3 and 4 should be powered in the same phase and have to be out of phase 180° toward ports 5 and 6.

It is shown in Fig. 6 that the strongest currents occur in the inner edge of the H-shaped slots are achieved and spread into wider track on cylinder surface. The surface currents of mode 1 flows in one direction on cylinder as shown in Fig. 7a. Furthermore, the surface currents of mode 7 flows in different direction between two slot pairs on cylinder as shown in Fig. 7b. These two modes have similar current distributions with the characteristic currents obtained from the TCM simulation as shown in Fig. 1 which have been discussed in the previous section.

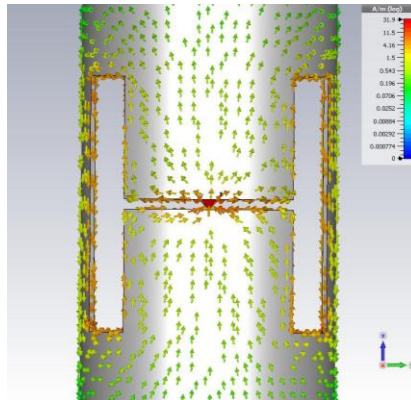


Fig. 6. Distribution current along the H-shaped slot.

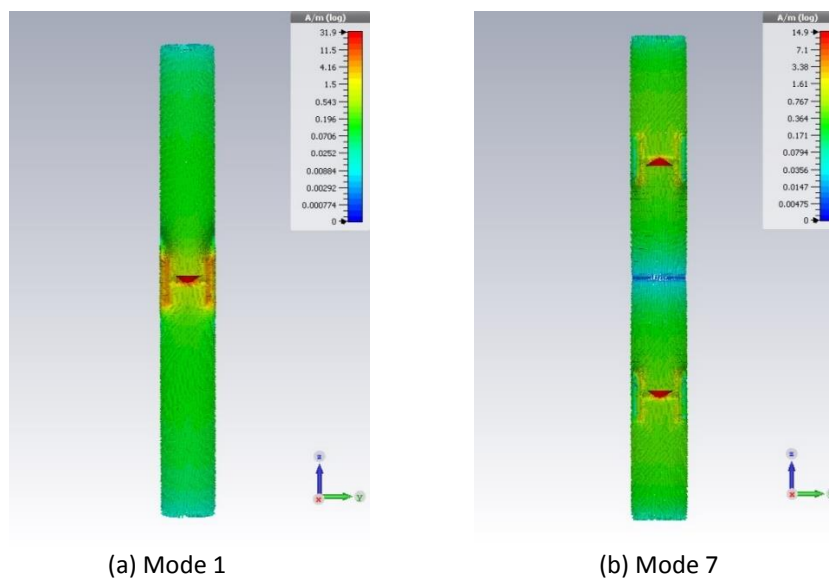


Fig. 7. Surface currents from simulation results.

5.2 Radiation Patterns

This master thesis also aims to obtain the desired radiation pattern of the cylinder. The mounting of the slots on cylinder determine its radiation pattern. Radiation pattern of each mode is achieved by conducting the simultaneous excitation. The simulation of mode 1 is performed by exciting two ports simultaneously which generates radiation pattern of omnidirectional as shown in Fig. 8a. The simulation of mode 7 is conducted by exciting two pairs of port simultaneously, with the different phase 180° between each pair of port. This mode 7 generates more directive radiation pattern that can be seen in Fig. 8b. They have similar results with characteristic field obtained from the TCM simulation in Fig. 1 above.

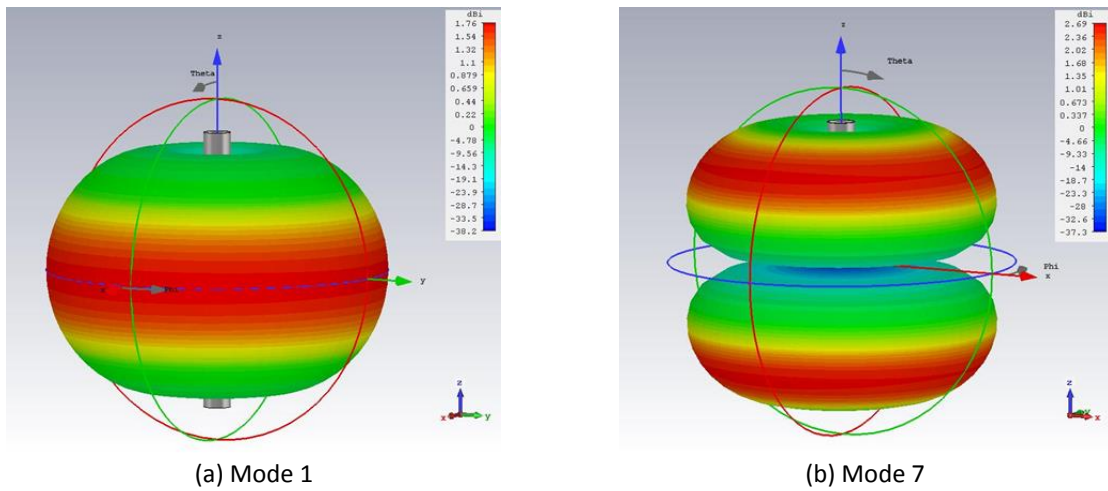


Fig. 8. Radiation Pattern of cylinder.

FEEDING SYSTEM OF SLOTS

The cylinder with slots are designed and simulated in the CST software. After that, feeding the slots is performed by firstly simulating it in the CST software before manufacturing. In designing the feeding of slots, the suitable matching networks are needed to be taken into account. By adding the lumped elements such as capacitors or inductors, can modify the impedance and bandwidth, without need further modification of structure [3]. Despite of reactive components, the cables that are used in the connection of matching networks can affect the input impedance as well. In this section, several possible feeding techniques are presented taking into account the cable length and suitable matching networks.

6.1 L-Matching Network

In practical, impedance matching of the cylinder ports to the input impedance has to be investigated. Simulation results show that, each cylinder ports in modes 1 and 7 have impedance of $Z_{ant,mode1} = 2.69 + j44.36 \Omega$ and $Z_{ant,mode2} = 17.39 + j129.22 \Omega$, respectively. These impedances should be matched to 50Ω in order to obtain S parameter $\ll -10$ dB. Before being implemented in the manufacturing, it will be better to calculate the matching networks for each mode in the simulation software. There is schematic tool in the CST simulation software which can be used to design the matching network interconnected to the antenna simulation result.

Matching networks are designed by using the lumped elements. There are eight possible L-matching networks that can be implemented. They are determined based on the application of the frequency use and antenna impedance. In the matching networks, several parameters such as input impedance, S parameter, and bandwidth can be investigated using design tools such as the smith chart. There are inductance part represent jX and conductance part represent $-jX$ in the chart. Designer of matching network enables to make impedance matching by adding capacitors and inductors in series and shunt combination. Fig. 9 depicts the component motions on the ZY chart [11]. Adding a capacitor to the network makes the direction of movement toward the lower part that eliminates the inductive reactance. Otherwise, an inductor that connected to the network makes the movement toward the higher part that can eliminate the capacitive reactance [11].

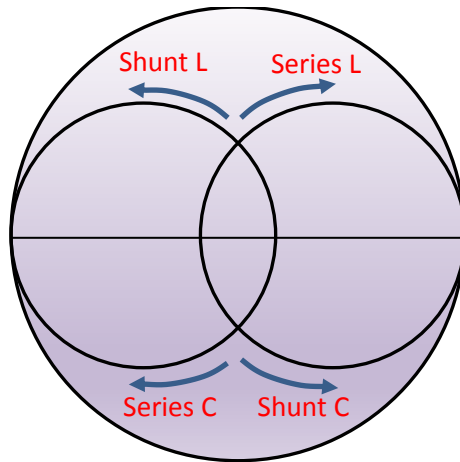


Fig. 9. Movement of adding reactive components on smith chart.

In the implementation, the different modes utilize the different L-matching network. It depends on cylinder impedance that requires to be matched. In the case of modes 1 and 7, their each ports having inductive character impedance that require to be excited. In order to match each of the cylinder impedance to 50Ω , there are four possible L-matching networks that can be implemented either for mode 1 or mode 7. Those L-matching networks are constructed of capacitors in shunt-series, capacitors in series-shunt, capacitor series-inductor shunt, and capacitor shunt-inductor series as shown in Fig. 10.

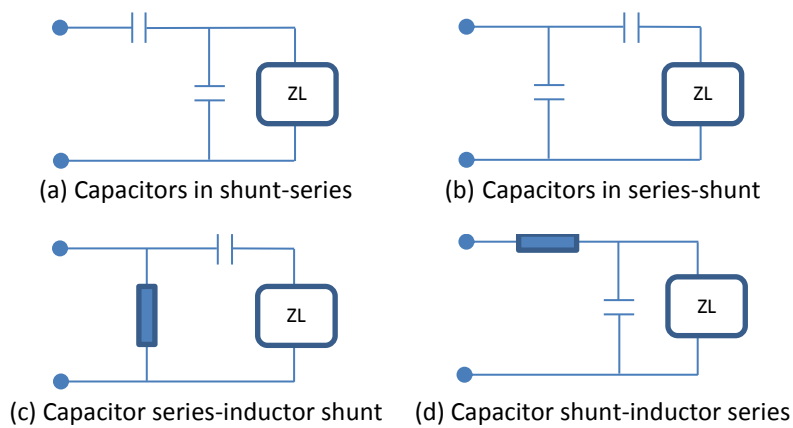


Fig. 10. Four possible matching network for modes 1 and 7.

6.2 Cable Impedance

When designing the L-matching networks, the parameter of cables that connect the cylinder to the matching networks or from the matching networks to the port should be taken into the calculation. Coaxial cable can be acted as transformer since this length can change the load impedance value. Thus, the impedance between input and output of cable will be different. It has been discussed in [12], input impedance of the cable is influenced by some parameters that given as:

$$Z_{IN} = Z_0 \frac{Z_L + jZ_0 \tan \beta L}{Z_0 + jZ_L \tan \beta L} \quad (7)$$

Where $\beta = 2\pi/\lambda_g = 2\pi\sqrt{\epsilon_r}/\lambda_0 = 2\pi f\sqrt{\epsilon_r}/c$, L is cable length, Z_0 is characteristic impedance, and Z_L is load impedance. ϵ_r denotes relative dielectric constant of the cable which has value 2.3 for RG58 coaxial cable type. When these parameters are modified, the input impedance of cable changes. Therefore, these cable parameters should be added into the calculation of matching networks in CST software using transmission line block.

In the transmission line, the ratio between the reflected and the incident wave is defined as the reflection coefficient. From the known input impedance, the reflection coefficient of cylinder feed can be determined by [13]:

$$\Gamma = \frac{Z_{IN} - Z_0}{Z_{IN} + Z_0} \quad (8)$$

When Γ is converted to dB, so called the S-parameter or return loss. Return loss in the matching networks denominates the power loss of the source over the load. It can be expressed in [13]:

$$RL(dB) = -20\log(|\Gamma|) \quad (9)$$

Furthermore, the relative bandwidth of cylinder is defined as the range frequencies within which the cylinder characteristic, such as input impedance and S-parameter, are in the acceptable value [14]. The relative bandwidth is given as [15]:

$$BW = \frac{f_2 - f_1}{\sqrt{f_1 f_2}} \quad (10)$$

Where f_2 and f_1 are the upper and lower frequency band for S-parameter of input cylinder below -10 dB, respectively. In addition, the quality factor of cylinder related to the bandwidth is given as [16]:

$$Q = \frac{1}{BW} \quad (11)$$

There are three schemes of implementation L-matching networks using cables. These schemes are designed by respecting the influence of the cable length towards the input impedance matching and desired relative bandwidth. Each scheme of matching network provides different results. These schemes use the concept of power divider, which power from the source is divided into two ports and four ports of cylinder in the case of modes 1 and 7, respectively. Further research related to this concept can be found regarding to the theory of Wilkinson power divider or N-way power divider in [17] and [18].

The first configuration is performed by connecting each cylinder port to its own matching circuit, then they are connected together to the feeding port using each cable with the same length. This configuration can be performed for mode 1 using four possible L-matching networks as shown in Fig. 11. The cable length is not become problem since with cable length 200 mm or longer, two capacitors L-matching networks can be used with value $C1 = 16 \text{ pF}$ in shunt and $C2 = 12 \text{ pF}$ in series.

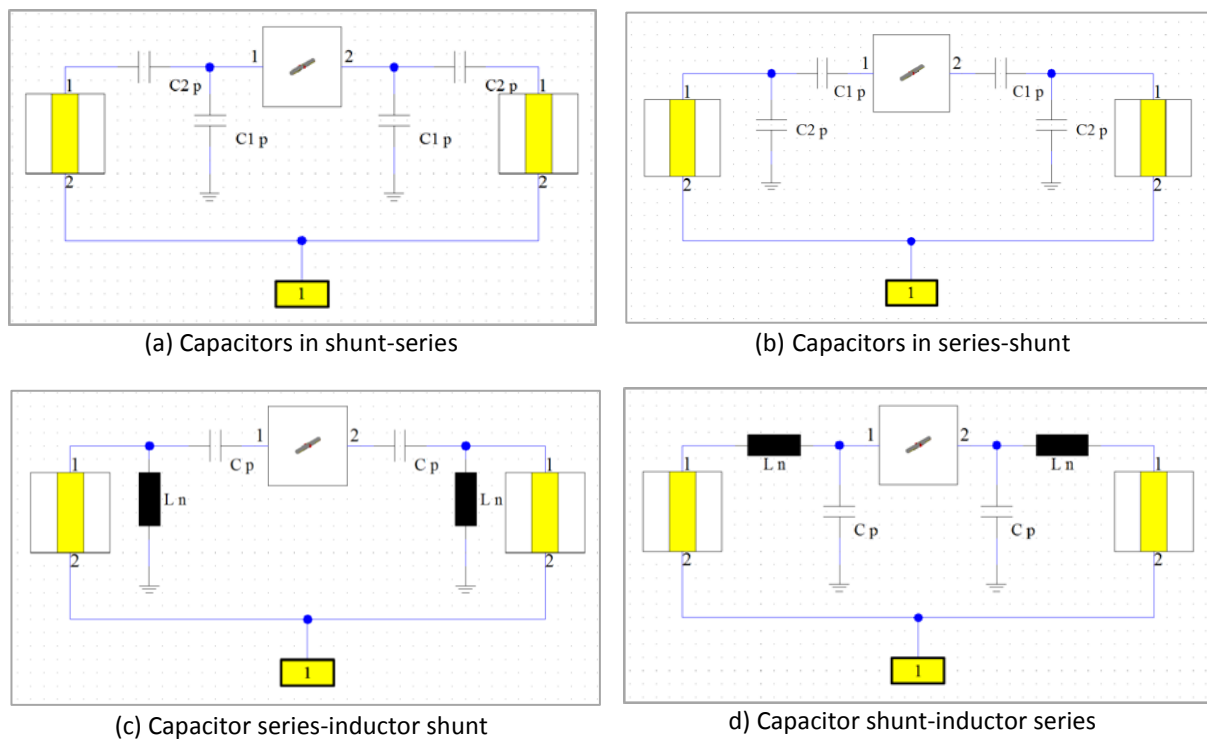


Fig. 11. First configuration of matching networks for mode 1.

Similar with mode 1, the first configuration can be realized for mode 7 using four possible L-matching networks as shown in Fig. 12. The cable length of 350 mm used in this mode is sufficient to be implemented in the manufacturing. Nevertheless, there are not many length of cable can be used for mode 7, the only cables with the length of 350 mm, 700 mm, and multiple of $\lambda_g/2$ can be used for all possible matching networks. For the frequency of 285MHz yields, $\frac{\lambda_g}{2} = \frac{\lambda_0}{2 \times \sqrt{2.3}} = \frac{1.052}{2 \times \sqrt{2.3}} = 346.80 \text{ mm} \approx 350 \text{ mm}$. When $\lambda_g/2$ of cable is used, the input impedance on smith chart will return to the initial position, while other cable lengths can

modify the input impedance. It means that the different cable lengths provide different effects to the impedance matching requiring other schemes of the matching networks.

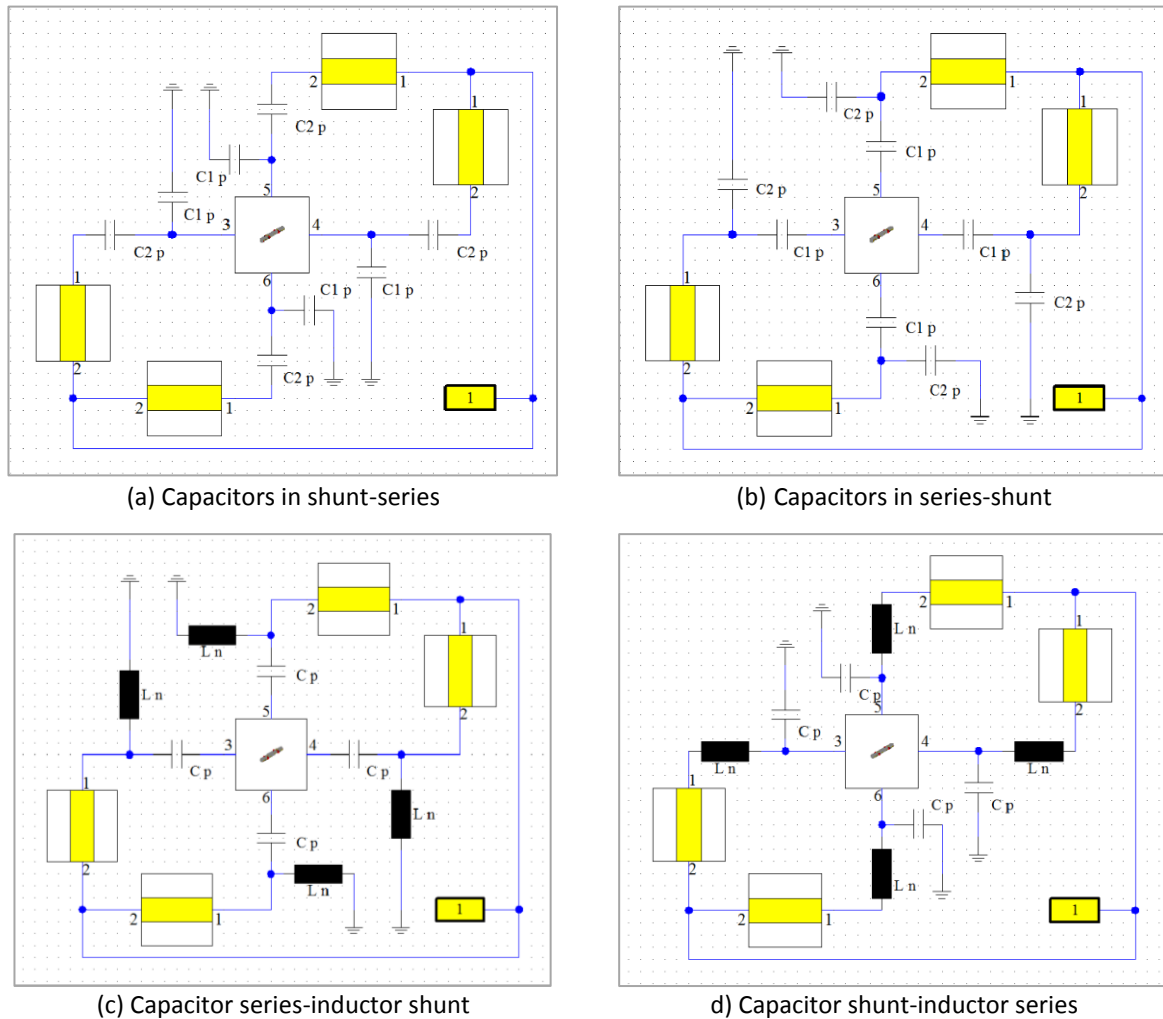


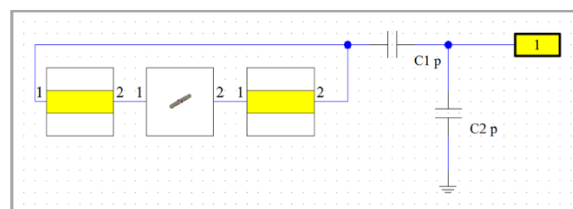
Fig. 12. First configuration of matching networks for mode 7.

Furthermore, the calculation results of the first configuration for given cable length and the capacitor value to get the desired S parameter can be seen from Table 5. For the excitation mode 1 using L-matching network with two capacitors in shunt-series, the cylinder has a good S-parameter -30.15 dB for frequency 126 MHz with frequency band for $S_{11} < -10$ dB of 122.02 – 130.71 MHz. Whereas for the excitation mode 7, cylinder has S-parameter -45.07 dB and the frequency band 265.84 – 300.08 MHz. The quality factor of cylinder either in mode 1 or mode 7 has high value that indicates the narrow bandwidth of both modes. In the TCM simulation, the cylinder has broadband bandwidth potential. However, in practical, the cylinder should be matched to the impedance 50Ω and hence the structure of matching network can affect the bandwidth of cylinder.

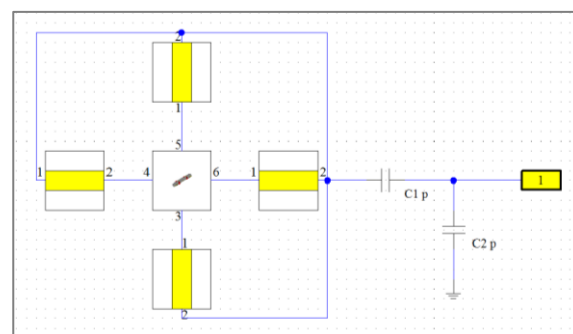
Table 5. Calculation value for excitation modes in the first configuration.

Mode	Cable Length [mm]	C1 [pF]	C2 [pF]	C [pF]	L [nH]	Input Impedance [Ω]	S-Parameter [dB]	Frequency Band [MHz]	BW	Q
1-a	200	16	12			$51.36 + j2.73$	-30.15	122.02 – 130.71	0,07	14,53
	300	15	12			$47.26 - j5.86$	-23.87	121.47 – 129.31	0,06	15,99
1-b	200	37	54			$51.27 + j2.68$	-31.85	122.27 – 130.69	0,07	15,01
	300	33	72			$47.35 - j0.45$	-32.67	121.66 – 130.11	0,07	14,89
1-c	200			19	18	$48.73 + j4.37$	-25.86	123.22 – 129.16	0,05	21,24
	300			20	15	$50.45 - j3.53$	-29.67	122.93 – 130.41	0,06	16,93
1-d	200			33	215	$48.42 - j1.64$	-31.84	122.99 – 129.00	0,05	20,96
	300			35	165	$50.44 + j0.25$	-33.35	123.12 – 128.73	0,04	22,44
7-a	350	2.4	4.5			$50.51 + j0.00$	-45.07	265.84 – 300.08	0,12	8,25
	700	2.3	5.2			$49.72 + j0.18$	-42.33	276.01 – 293.19	0,06	16,56
7-b	350	20	4			$51.32 - j0.34$	-37.26	267.46 – 297.53	0,11	9,38
	700	18	3.7			$49.04 + j0.71$	-36.85	276.56 – 292.24	0,06	18,13
7-c	350			2.6	68	$52.26 + j0.35$	-32.60	275.58 – 295.18	0,07	14,55
	700			2.6	64	$52.36 - j0.02$	-31.77	279.15 – 291.33	0,04	23,41
7-d	350			5	90	$52.02 - j1.47$	-32.11	270.90 – 296.65	0,09	11,01
	700			5	100	$53.06 - j3.24$	-27.22	277.32 – 291.75	0,05	19,71

In the second configuration, each cylinder port is connected to its matching network by cable with the same length. This order is implemented for modes 1 and 7 as shown in Figs. 13a and 13b, respectively.



(a) mode 1



(b) mode 7

Fig. 13. Second configuration of matching networks.

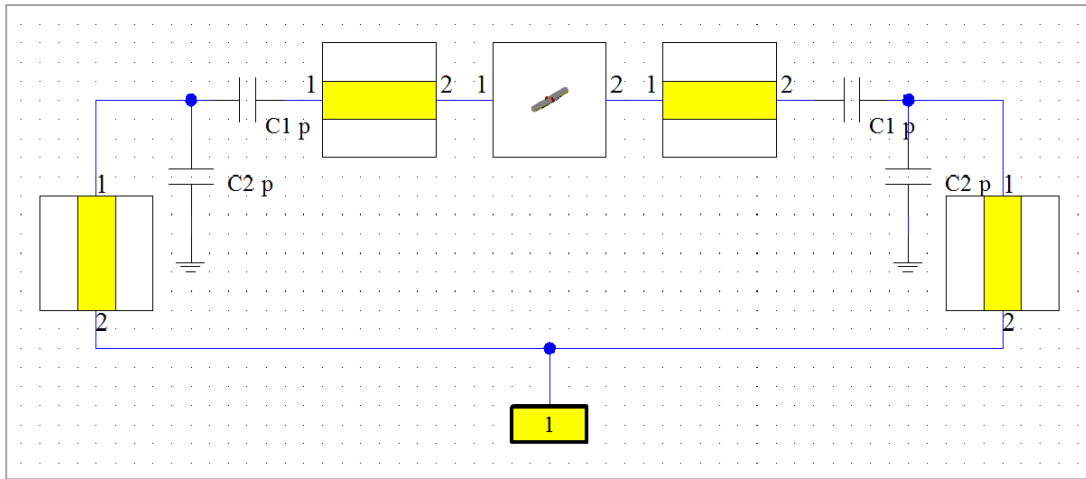
The second configuration is trivial to be implemented in the manufacturing. However, there is one point must be considered. If two capacitors want to be used in L-matching network in series-shunt, the length of each cable that can be used should be not longer than 150 mm and 350 mm for mode 1 and mode 7, respectively. It can be occurred since the load impedance

moves to the inside of $1+jX$ circle, in which two capacitors L-matching networks can not be used to match this load impedance. In the manufacturing, these lengths are sufficient that respect to the diameter of cylinder. It should be noted that longer length of cables are possible to be utilized only for multiple of $\lambda_g/2$, however it can reduce the bandwidth. Furthermore, the calculation between the capacitor values and the input impedance toward the cable length are shown in the Table 6. Due to its limitation, this configuration is not further discussed.

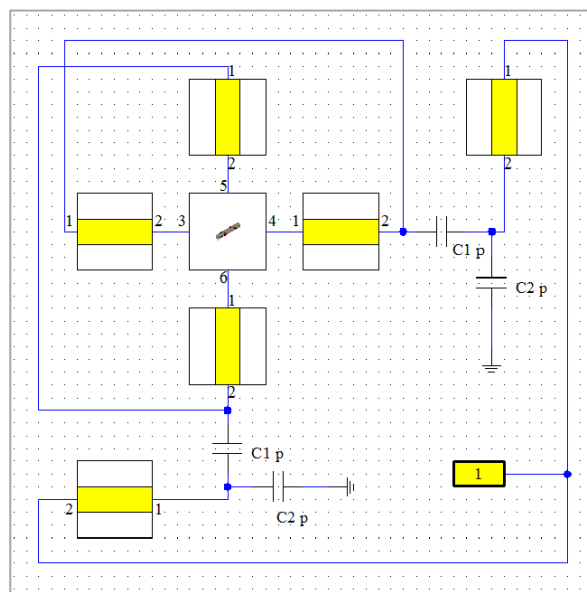
Table 6. Calculation value for excitation modes in the second configuration

Mode	Cable Length [mm]	C1 [pF]	C2 [pF]	Input Impedance [Ω]	S-parameter [dB]	Frequency Band [MHz]	BW	Q
1	150	12	16	$50.99 + j0.12$	-32.86	122.56 – 129.48	0,05	18,20
	850	44	75	$48.61 + j2.34$	-31.03	125.15 – 127.11	0,02	64,35
7	350	68	15	$50.79 + j2.18$	-32.41	276.07 – 292.93	0,06	16,87
	700	14	55	$49.77 - j1.09$	-40.32	280.48 – 289.23	0,03	32,55

Any of the required longer cable design in the manufacturing can utilize the third configuration. This scheme is depicted in Fig. 14. By using this configuration, the designer can apply any longer cable after the two capacitors L-matching circuit (i.e., second cable) with still consider the multiple of $\lambda_g/2$ cable length of mode 7. It can be seen from Table 7 that in this configuration, the use of any longer cable does not reduce the relative bandwidth of cylinder. Therefore, the third configuration can be implemented in the manufacturing.



(a) Mode 1



(b) Mode 7

Fig. 14. Third configuration of matching networks.

Table 7. Calculation value for excitation modes in the third configuration

Mode	1 st Cable [mm]	2 nd Cable [mm]	C1 [pF]	C2 [pF]	Input Impedance [Ω]	S-parameter [dB]	Frequency Band [MHz]	BW	Q
1	100	500	12	53	$47.73 - j0.47$	-31.67	122.11 – 130.15	0,06	15,68
	100	700	14	36	$45.68 - j2.37$	-25.39	123.19 – 129.07	0,05	21,44
7	350	700	33	7	$50.32 + j2.47$	-32.1	278.95 – 290.77	0,04	24,09
	350	1000	25	11	$47.48 - j0.1$	-31.11	278.37 – 290.28	0,04	23,87

MANUFACTURING OF PROPOSED DESIGN AND MEASUREMENT

The proposed design of cylinder having slots has been simulated and investigated. After that, the cylinder is fabricated and then the input impedance of this cylinder is measured in order to validate the simulation results. The manufacturing of cylinder is conducted for the first mode of cylinder as shown in Fig. 4a above.

7.1 Fabricated Cylinder

The fabricated cylinder is constructed from pipe made from steel with diameter 100 mm and length 1 m. The manufacturing process is including the cutting of slots and the soldering of capacitors and coaxial cable on the pipe. Process of cutting the slots is done manually by hand using cutting equipment. Even though fabricated by hand-made manufacturing, the slots have as precisely shape and dimension as from the simulation that can be seen from Fig. 15.



Fig. 15. Fabricated cylinder.

After cutting the slots, the next process is to implement the matching circuit into the pipe. This matching network follows the design in Fig. 11a above. It is constructed by soldering capacitors

15 pF in parallel and capacitors 12 pF in series with coaxial cable RG58C/U on the edge slots of pipe. The two matching networks from each slot are connected together by using coaxial cable to one sma connector. The detailed view of real configuration is shown in Fig. 16.

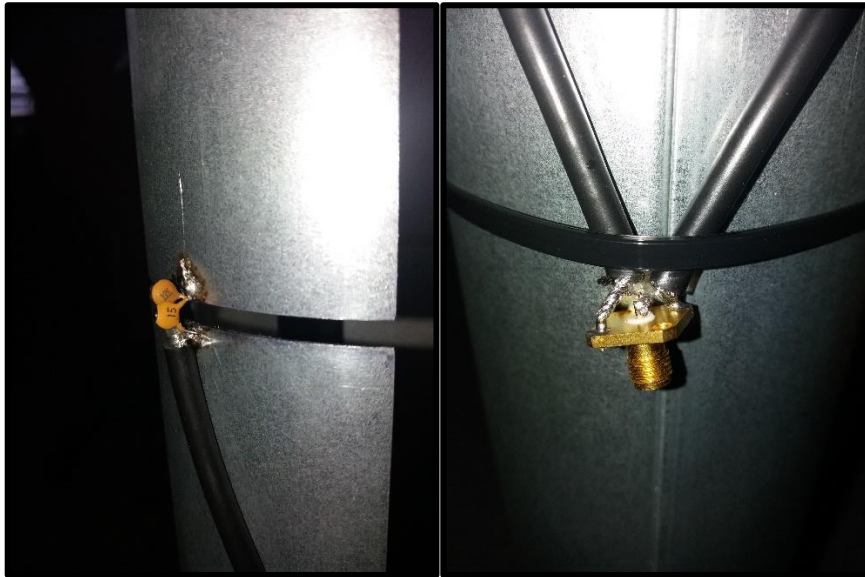


Fig. 16. Soldering of capacitors and coaxial cables.

7.2 Measurement of Fabricated Cylinder

After manufacturing process, the S-parameter and impedance of constructed cylinder are measured in the anechoic chamber as shown in Fig. 17. The measurement results show that fabricated cylinder has good S11 of -20.11 dB for frequency 126 MHz with the frequency band of 121 MHz – 130.2 MHz. These results have very good agreement compared to the simulation, despite the value of S11 in simulation is -30,15 dB for the same frequency. Beside that, there is a very small peak appeared on the higher frequency in the measurement result, while do not appear in the simulation. It can be caused by the fact that the fabricated cylinder is not able as perfect as the simulation model, such as the soldering of capacitors and cable that need some wires. Note that the capacitors 15 pF soldered on the pipe have 1 pF less than in the simulation, i.e., 16 pF. However, the capacitors have tolerance of 5%, therefore the value of capacitors can be higher or lower. Fig. 18 shows the comparison of S-parameter values between simulation and measurement results. Input impedance of cylinder from the measurement is $55.44 - j8.92 \Omega$, while from the simulation is $51.36 + j2.73 \Omega$. The Q factor of cylinder from measurement is 13.64 that show the bandwidth of fabricated cylinder is little bit wider than the simulation with the Q factor of 14.53.

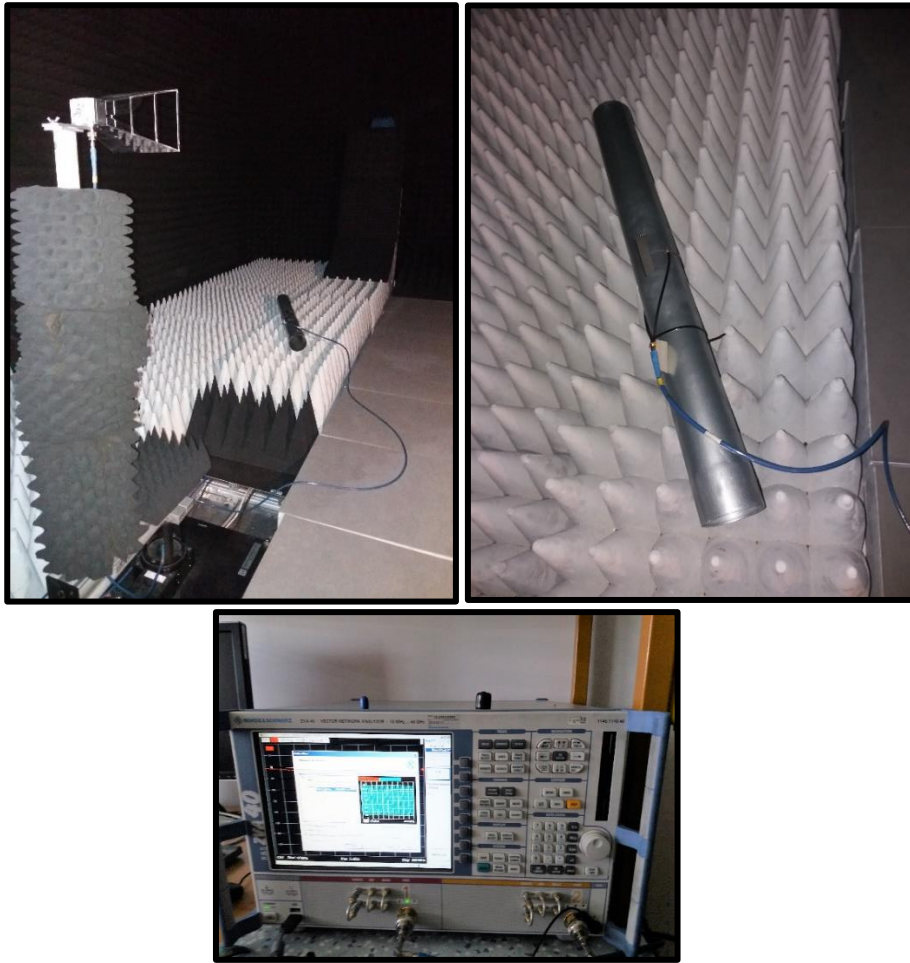


Fig.17. Measurement of fabricated cylinder in the anechoic chamber.

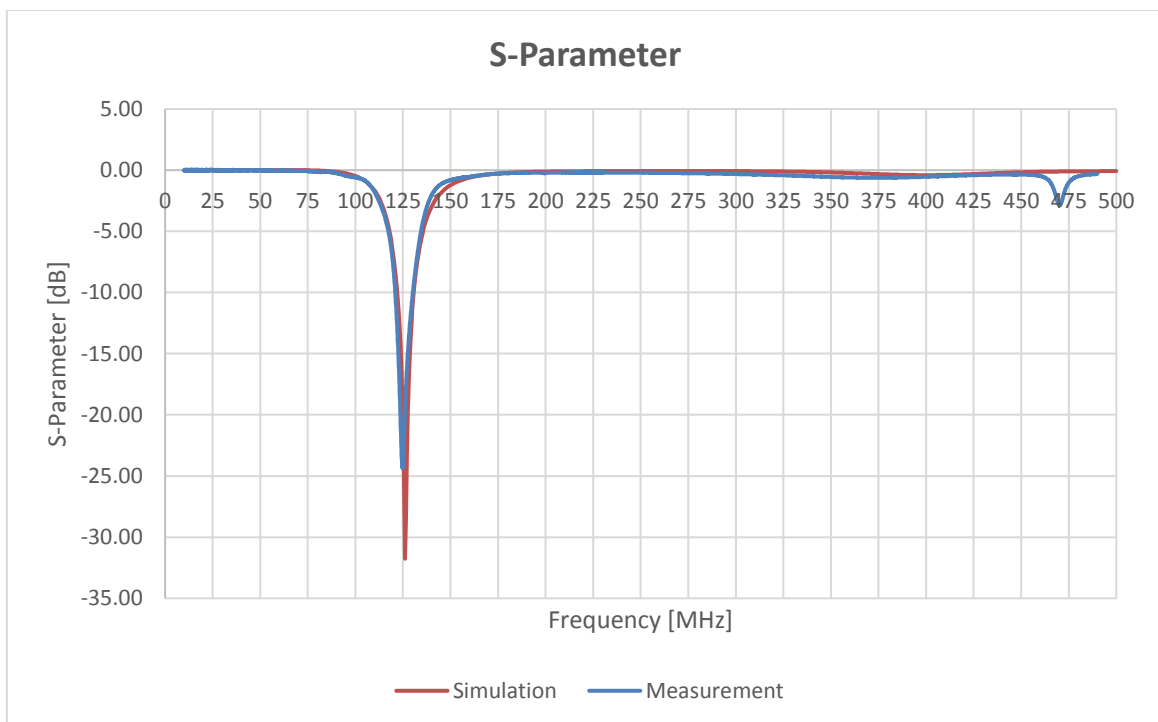


Fig. 18. S-Parameter results between simulation and measurement.

Chapter 8

CONCLUSION

This master thesis deals with the investigation of the excitation of the rocket chassis as an effective radiator. The theory of characteristic mode (TCM) is used to find the resonance modes of the cylinder of rocket. For the simulation purpose, the model of rocket of conducting cylinder is designed using FEKO software. The simulation results show that the cylinder of rocket behaves like a dipole. The cylinder have similar characteristic currents to a dipole. However, its lower resonant frequency represents a thicker dipole. Since the modes have characteristic currents with minimum and maximum at the specific location, the effective way to excite the modes is by utilizing the inductive coupler elements that are mounted at the maximum currents.

Furthermore, the excitation of the conducting cylinder having slots is performed by using CST software. For simulation purposes, the PEC cylinder with the length of 1 m and the diameter of 0.1 m are designed. There are two selected modes that are excited on the cylinder by utilizing the H-shaped slots. Note that the designed H-shaped slot can obtain the higher real part impedance compared to other shapes. Then, the excitation of mode 1 is performed by exciting two slots in phase, while the excitation of mode 7 is conducted by exciting two of four slots in phase and the other two are 180° out of phase. From the simulation results, the cylinder has a similar results of surface currents and radiation pattern compared to the TCM simulation results. All of this show that the excitation cylinder using mounted H-shaped slots to achieve the desired modes is proven.

After the cylinder with slots are designed and simulated in the CST software, the design of the feeding system of the slots is performed by firstly simulating it in the CST software before the manufacturing. In designing the feeding of slots, the suitable matching networks and coaxial cable parameters are required to be taken into account in order to match the cylinder impedance to 50Ω . The configuration of matching network and coaxial cable can affect the bandwidth. There are four possible L-matching networks that can be implemented to both modes for the given load impedance. Furthermore, there are three schemes of implementation the feeding slots by considering these L-matching networks and cable length. They are determined based on the application of the resonant frequency and the obtained input impedance of cylinder. In the matching networks, several parameters such as the input impedance, S-parameter, and bandwidth are investigated and optimized by using the design tools of smith chart in CST software. In addition, the quality factor of cylinder either in mode 1 or mode 7 has high value that indicate the narrow bandwidth of both modes. Even though the cylinder has broadband bandwidth potential in the TCM simulation, however in practical the cylinder should be matched to the input impedance. Hence, the implementation of matching networks limits the bandwidth very much.

The proposed design of the cylinder having slots is fabricated. Then, the input impedance of this cylinder is measured in the anechoic chamber. The manufacturing of cylinder is conducted

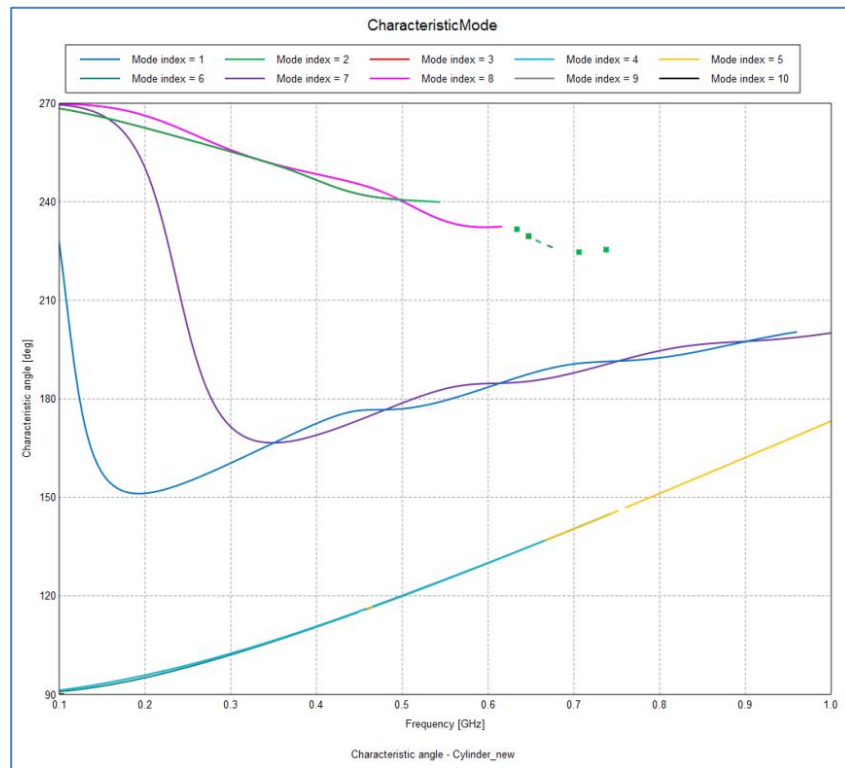
only for mode 1. It is shown that the measurement results of the fabricated cylinder have excellent agreement conforming to the simulation results. Actually, it is possible to excite mode 7 as well based on the simulation results. However, it faces complicated process of cutting the slots, thus the manufacturing of cylinder using mode 7 is not conducted. Nevertheless, the fabricated cylinder using mode 1 is sufficient to show that the excitation of conducting cylinder is working very well.

For further research, it is interesting to investigate how the different dimension of cylinders perform the different modes and evaluate the excitation modes for higher frequency. Also, the implementation of better design of matching networks to obtain the wider bandwidth can be examined in the future works.

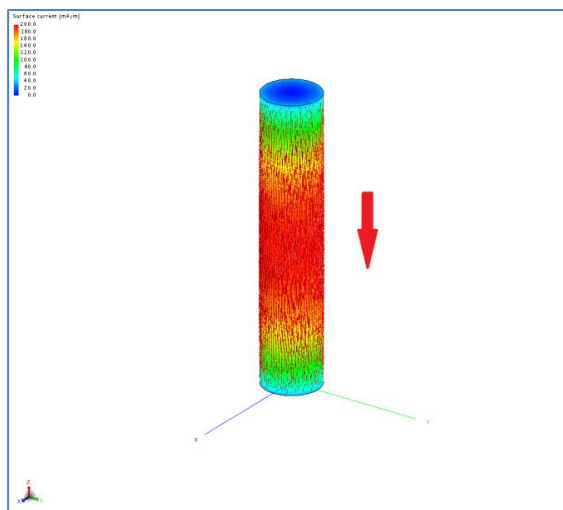
REFERENCES

- [1] R. J. Garbacz, "A generalized expansion for radiated and scattered fields," Ph.D. dissertation, The Ohio State Univ., 1968.
- [2] R. F. Harrington and J. R. Mautz, "Theory of characteristic modes for conducting bodies," *IEEE Trans. Antennas Propag.*, vol. 19, no. 5, pp. 622–628, Sept. 1971.
- [3] Y. Chen and C.-F. Wang, *Characteristic Modes – Theory and Applications In Antenna Engineering*. John Wiley, 2015.
- [4] <http://www.feko.info/>
- [5] <https://www.cst.com/>
- [6] Cabedo-Fabres, E. Antonino-Daviu, A. Valero-Nogueira, and M. F. Bataller, "The theory of characteristic modes revisited: A contribution to the design of antennas for modern applications," *IEEE Antennas Propag. Magazine*, vol. 49, no. 5, pp. 52–68, Oct. 2007.
- [7] R. Martens, E. Safin, D. Manteuffel, "Inductive and capacitive excitation of the characteristic modes of small terminals", *Proc. LAPC*, pp. 1-4, Nov. 2011.
- [8] R. F. Harrington and J. R. Mautz, "Control of radar scattering by reactive loading," *IEEE Trans. Antennas Propag.*, vol. 20, no. 4, pp. 446–454, July 1972.
- [9] R. Martens, E. Safin, D. Manteuffel, "Selective Excitation of Characteristic Modes on Small Terminals," *EUCAP 2011*, Roma, pp. 2492 – 2496, April 2011.
- [10] R. Martens, D. Manteuffel, "A feed network for the selective excitation of specific characteristic modes on small terminals", *6th European Conference on Antennas and Propagation (EUCAP) 2012*, pp. 1842-1846, 2012.
- [11] E. Abdullah, *Introduction to RF Power Amplifier Design and Simulation*. CRC Press, 2016.
- [12] S. J. Orfanidis, *Electromagnetic Waves and Antennas*. ECE Rutgers University, 2016.
- [13] A. Grebennikov, N. Kumar, and B. S. Yarman, *Broadband RF and Microwaves Amplifiers*. CRC Press, 2016.
- [14] C. A. Balanis, *Antenna Theory*. Jhon Wiley & Sons, 2005.
- [15] P. Hazdra and M. Mazanek, *Basics of Radiation and Antennas*. FEE CTU in Prague, 2015.
- [16] J. L. Volakis, *Antenna Engineering Handbook*. McGraw-Hill, 2007.
- [17] E. J. Wilkinson, "An N-way hybrid power divider", *IRE Trans. Microw. Theory Tech.*, vol. MTT-8, pp. 116-118, Jan. 1960.
- [18] D. M. Pozar, *Microwave Engineering*. Jhon Wiley & Sons, 2012.

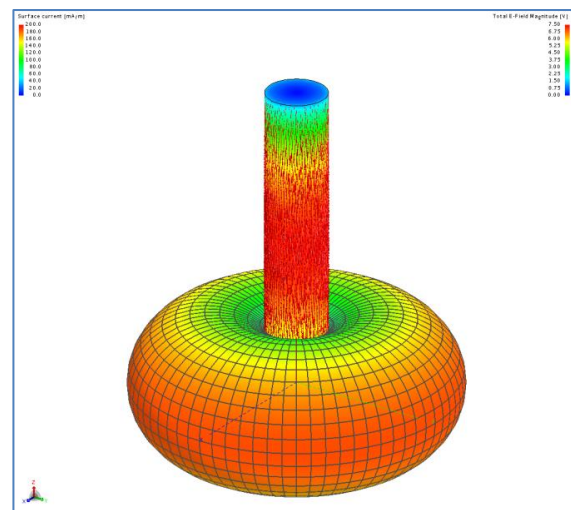
APPENDIX



Ap. 1 Variation of the characteristic angle with frequency, for the first ten characteristic modes of the closed cylinder with diameter 0.1 m and length 1 m.

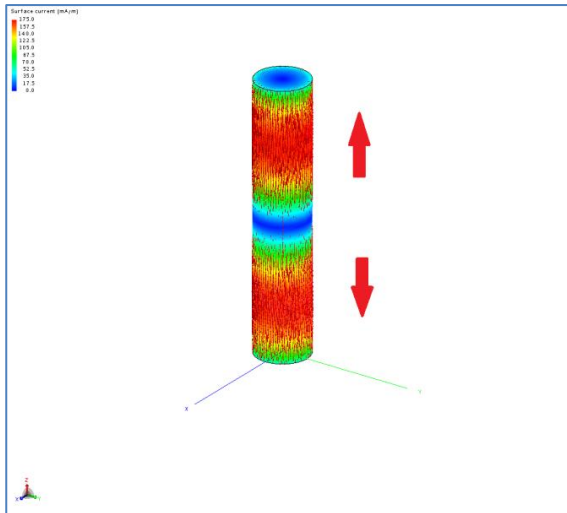


(a) Current distribution of mode 1.

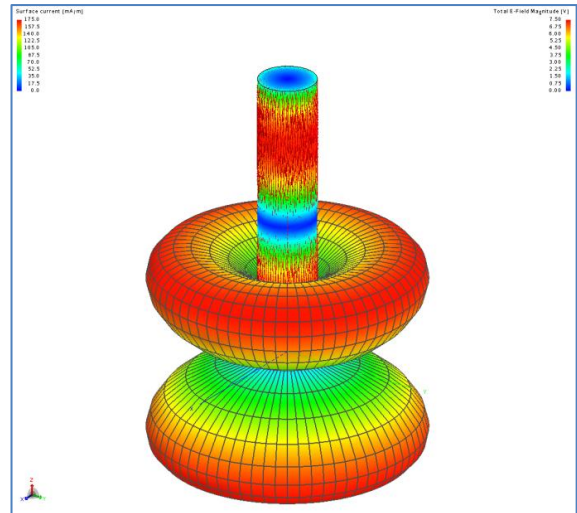


(b) Electric fields of mode 1.

Ap. 2 Characteristic mode 1 of the closed cylinder with diameter 0.1 m and length 1 m, resonant frequency 123 MHz.

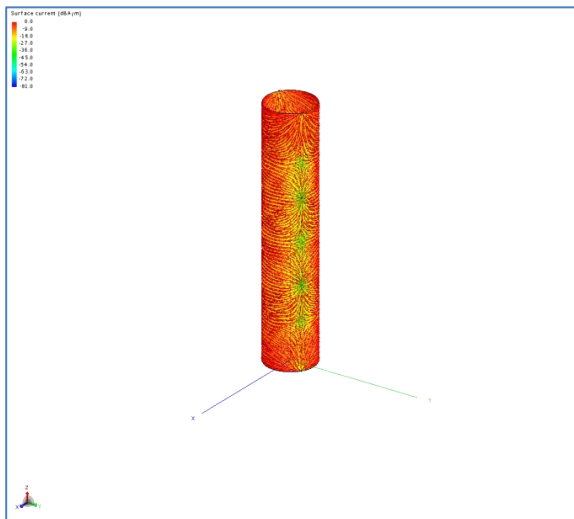


(a) Current distribution of mode 7.

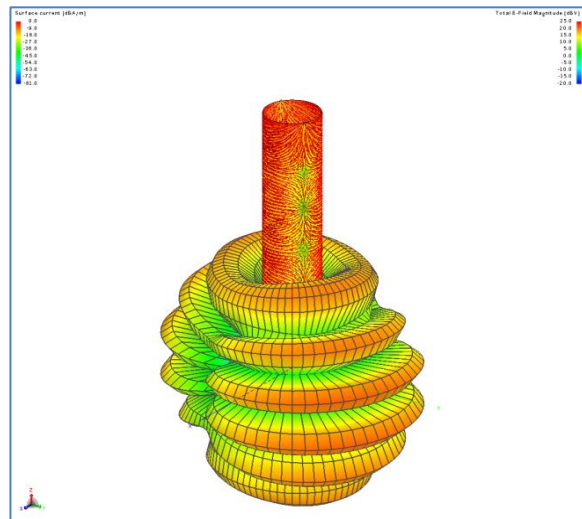


(b) Electric fields of mode 7.

Ap. 3 Characteristic mode 7 of the closed cylinder with diameter 0.1 m and length 1 m, resonant frequency 277 MHz.

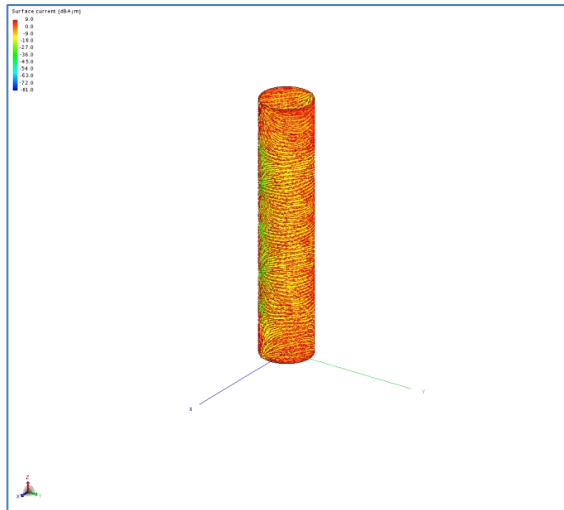


(a) Current distribution of mode 2.

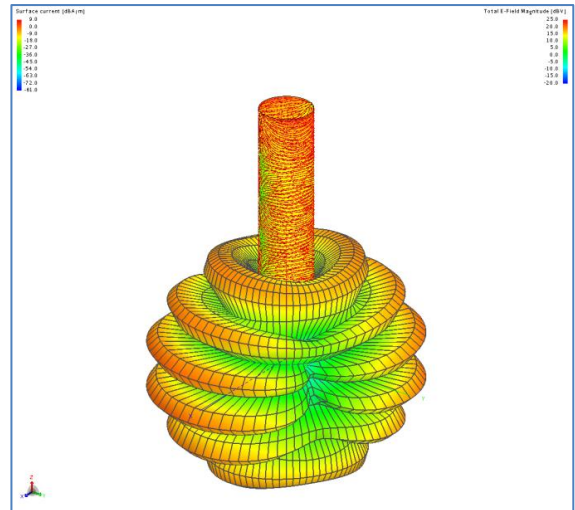


(b) Electric fields of mode 2.

Ap. 4 Characteristic mode 2 of the open cylinder with diameter 0.1 m and length 1 m, resonant frequency 872 MHz.

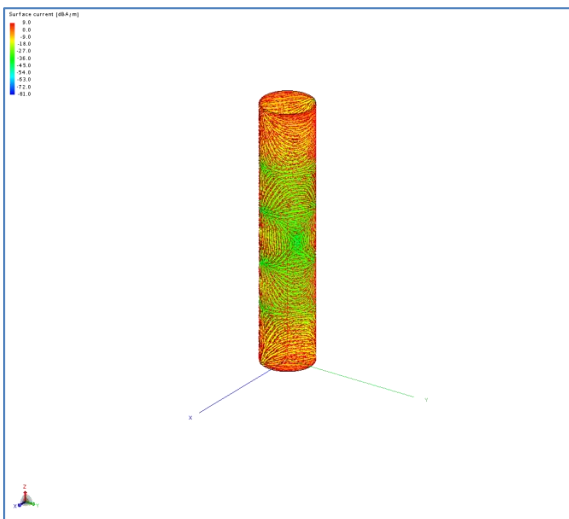


(a) Current distribution of mode 3.

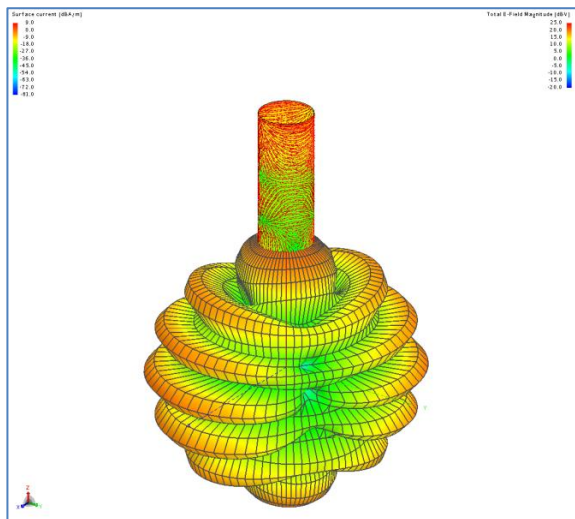


(b) Electric fields of mode 3.

Ap. 5 Characteristic mode 3 of the open cylinder with diameter 0.1 m and length 1 m, resonant frequency 872 MHz.

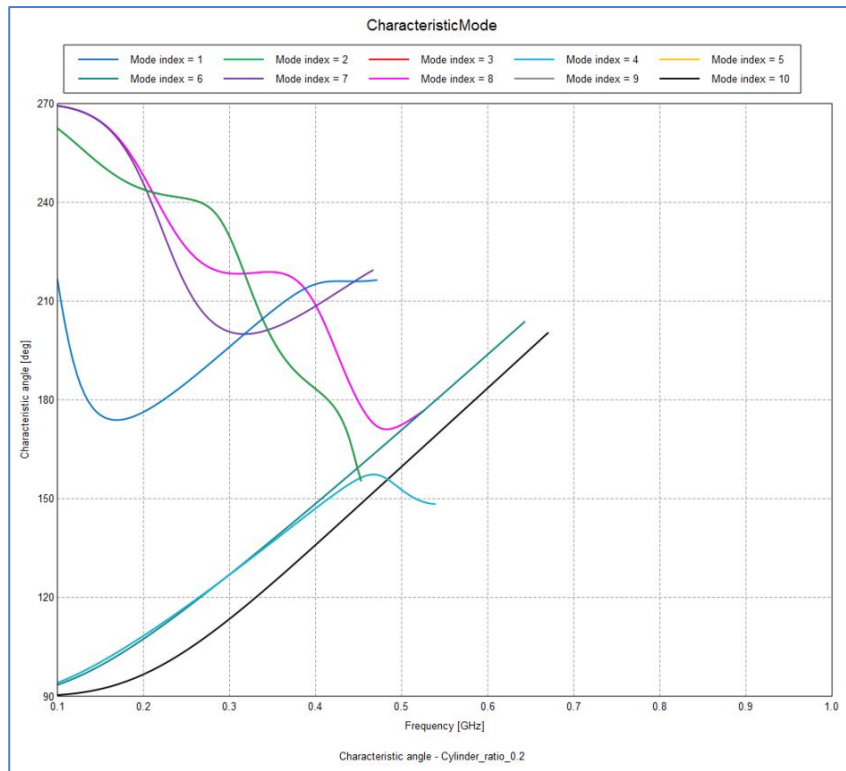


(a) Current distribution of mode 9.

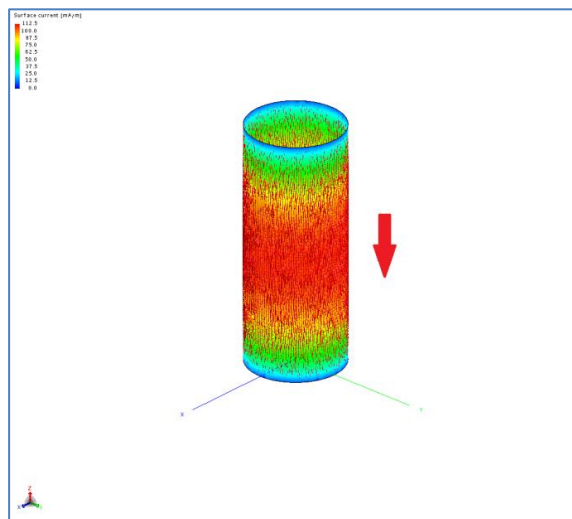


(b) Electric fields of mode 9.

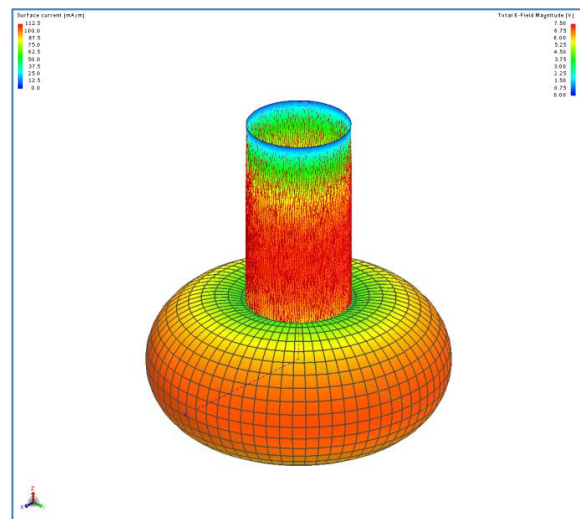
Ap. 6 Characteristic mode 9 of the open cylinder with diameter 0.1 m and length 1 m, resonant frequency 841 MHz.



Ap. 7 Variation of the characteristic angle with frequency, for the first ten characteristic modes of the open cylinder with diameter 0.2 m and length 1 m.

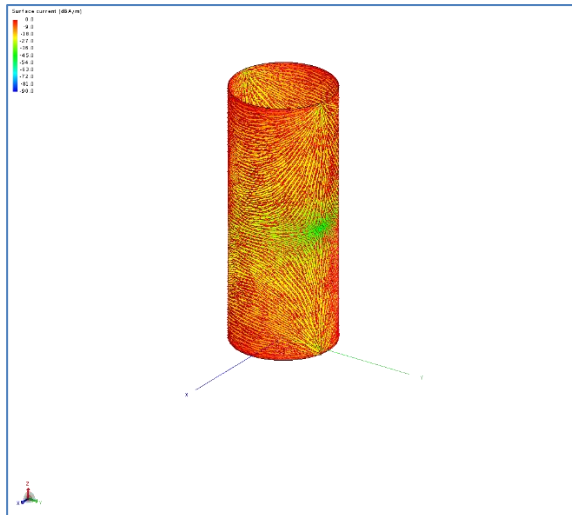


(a) Current distribution of mode 1.

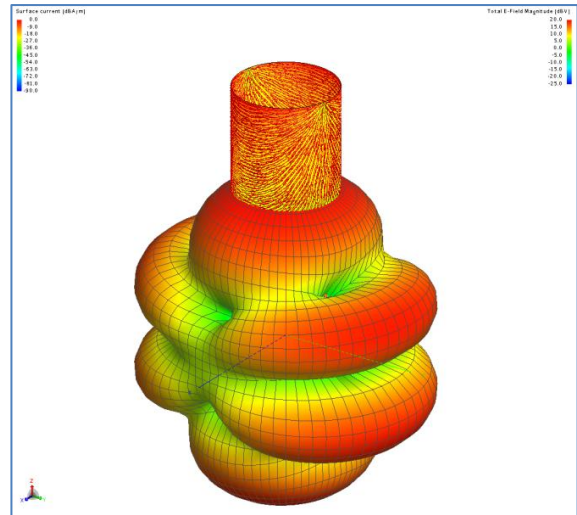


(b) Electric fields of mode 1.

Ap. 8 Characteristic mode 1 of the open cylinder with diameter 0.2 m and length 1 m, resonant frequency 134 MHz.

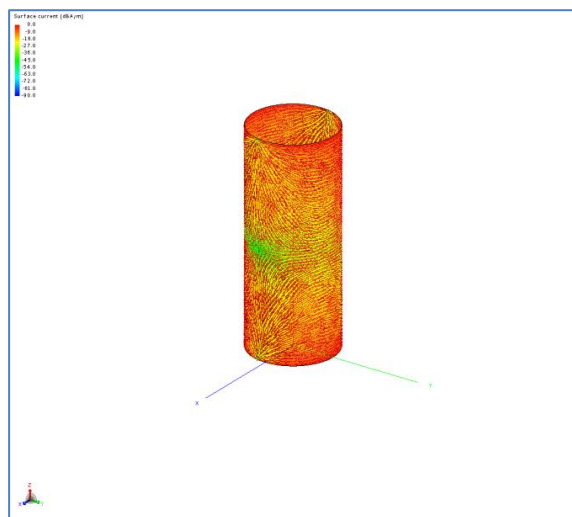


(a) Current distribution of mode 2.

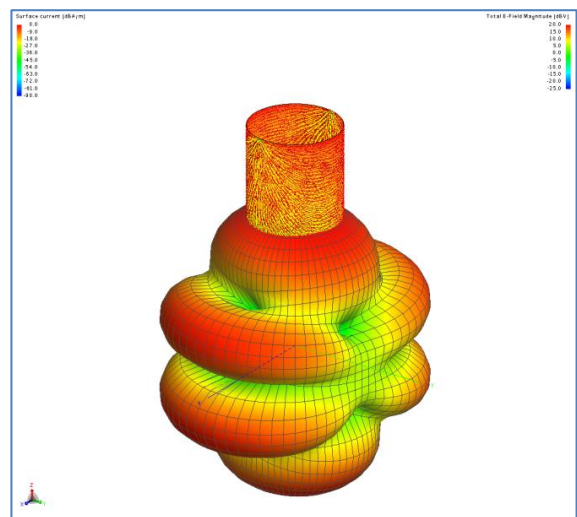


(b) Electric fields of mode 2.

Ap. 9 Characteristic mode 2 of the open cylinder with diameter 0.2 m and length 1 m, resonant frequency 414 MHz.

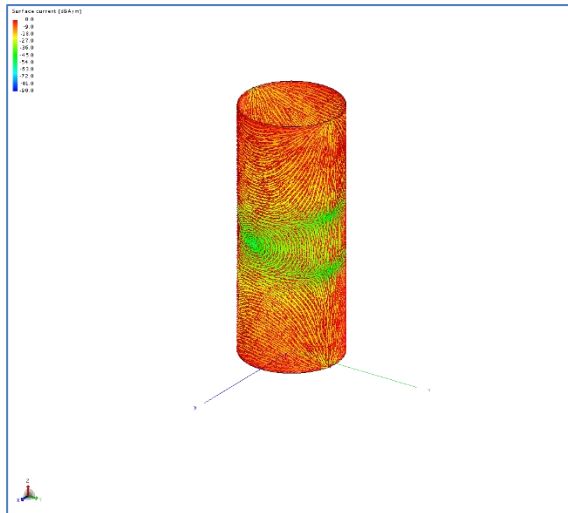


(a) Current distribution of mode 3.

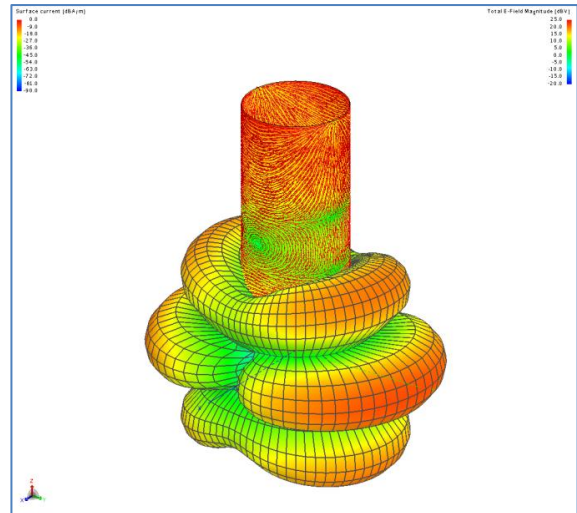


(b) Electric fields of mode 3.

Ap. 10 Characteristic mode 3 of the open cylinder with diameter 0.2 m and length 1 m, resonant frequency 414 MHz.

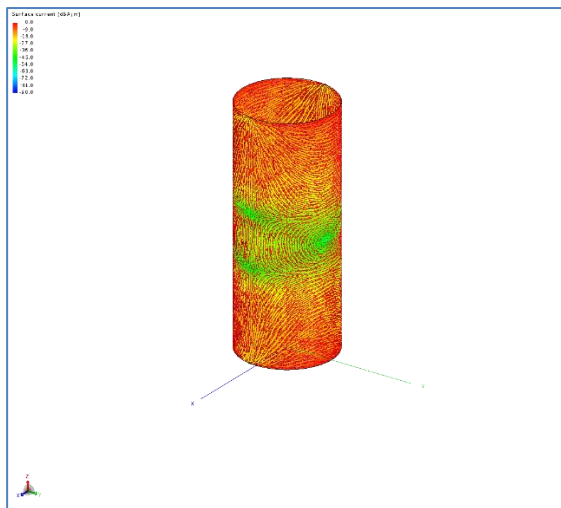


(a) Current distribution of mode 8.

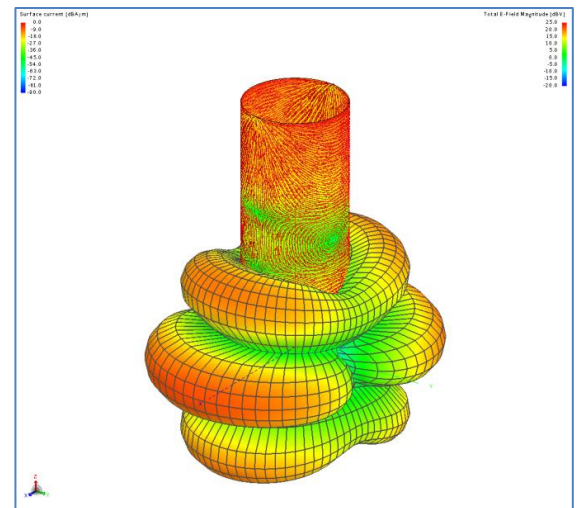


(b) Electric fields of mode 8.

Ap. 11 Characteristic mode 8 of the open cylinder with diameter 0.2 m and length 1 m, resonant frequency 448 MHz.

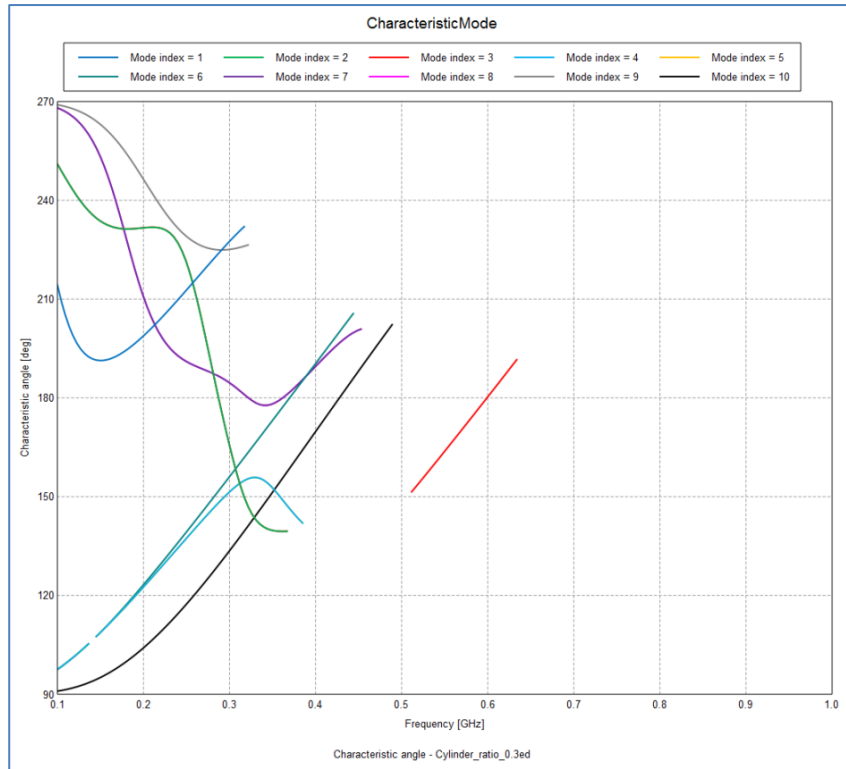


(a) Current distribution of mode 9.

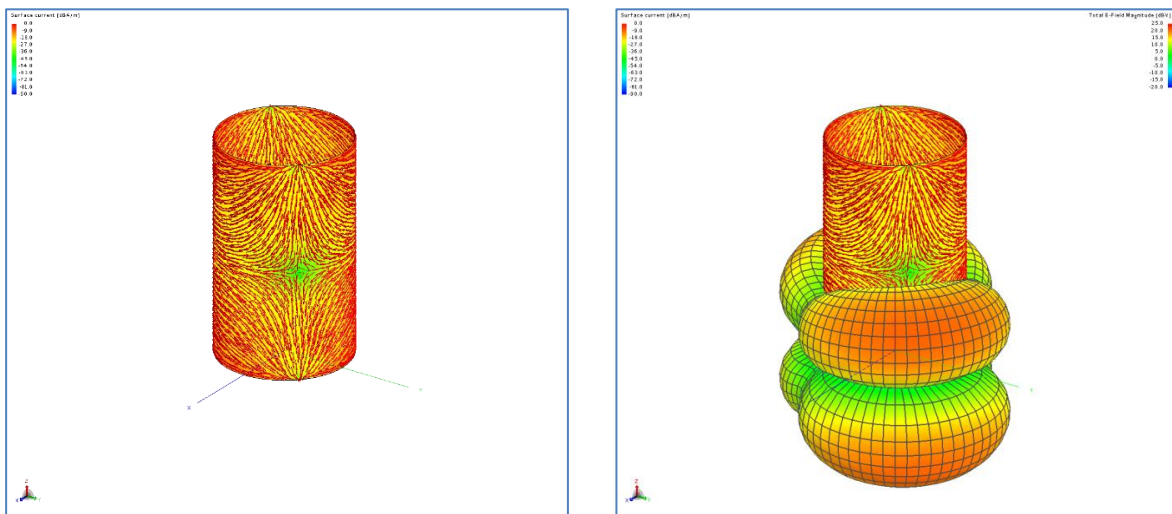


(b) Electric fields of mode 9.

Ap. 12 Characteristic mode 9 of the open cylinder with diameter 0.2 m and length 1 m, resonant frequency 449 MHz.



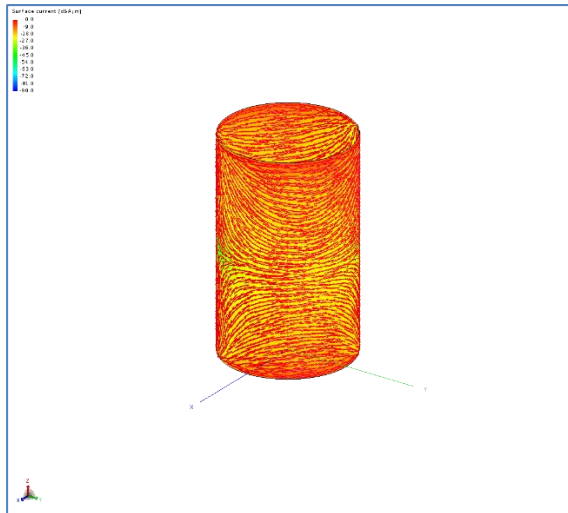
Ap. 13 Variation of the characteristic angle with frequency, for the first ten characteristic modes of the open cylinder with diameter 0.3 m and length 1 m.



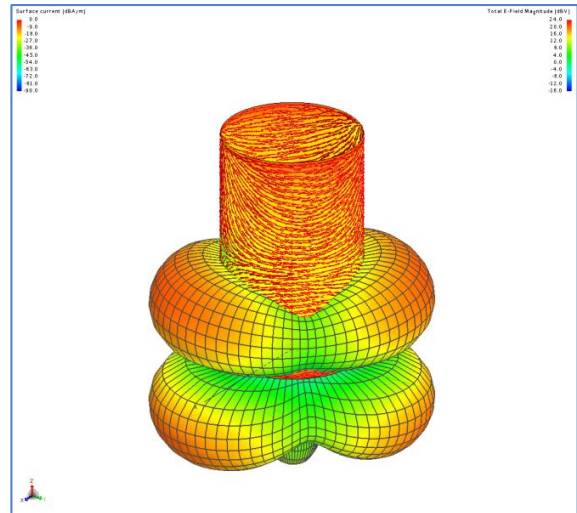
(a) Current distribution of mode 2.

(b) Electric fields of mode 2.

Ap. 14 Characteristic mode 2 of the open cylinder with diameter 0.3 m and length 1 m, resonant frequency 287 MHz.

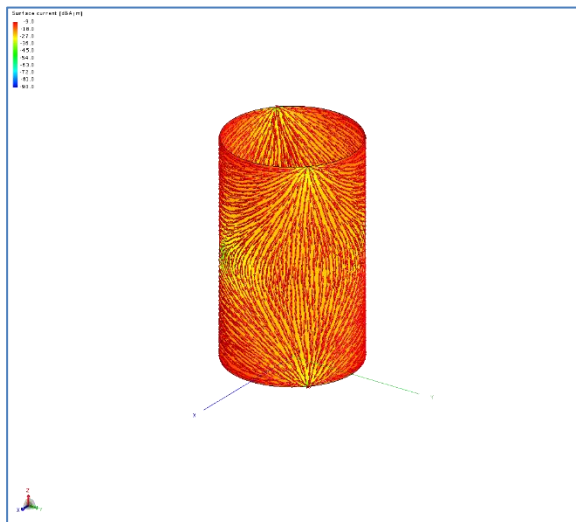


(a) Current distribution of mode 3.

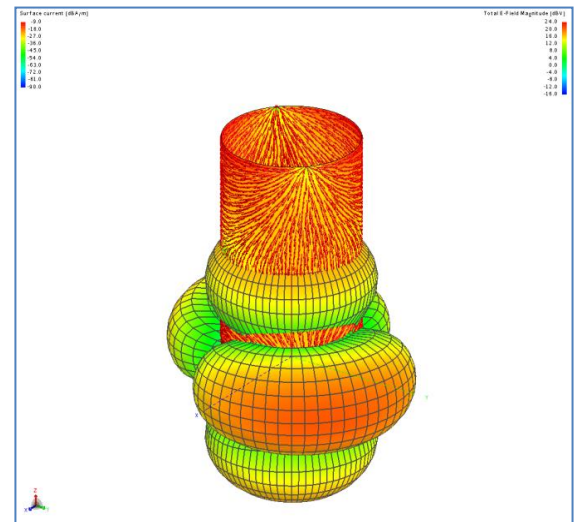


(b) Electric fields of mode 3.

Ap. 15 Characteristic mode 3 of the open cylinder with diameter 0.3 m and length 1 m, resonant frequency 287 MHz.

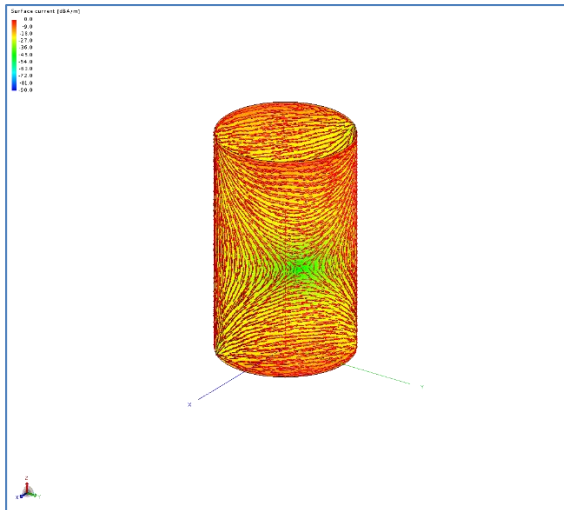


(a) Current distribution of mode 7.

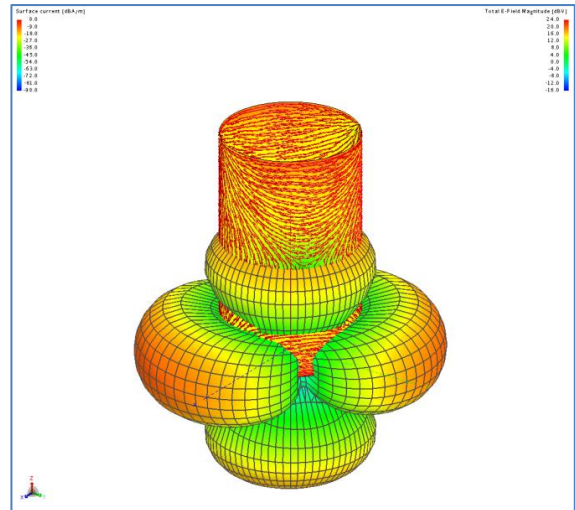


(b) Electric fields of mode 7.

Ap. 16 Characteristic mode 7 of the open cylinder with diameter 0.3 m and length 1 m, resonant frequency 321 MHz.



(a) Current distribution of mode 8.



(b) Electric fields of mode 8.

Ap. 17 Characteristic mode 8 of the open cylinder with diameter 0.3 m and length 1 m, resonant frequency 321 MHz.